40S subunit dissociation and proteasome-dependent RNA degradation in nonfunctional 25S rRNA decay.

AUTHOR(S):

Fujii, Kotaro; Kitabatake, Makoto; Sakata, Tomoko; Ohno, Mutsuhito

CITATION:

Fujii, Kotaro ...[et al]. 40S subunit dissociation and proteasome-dependent RNA degradation in nonfunctional 25S rRNA decay.. The EMBO journal 2012, 31(11): 2579-2589

ISSUE DATE:

2012-05-30

URL:

http://hdl.handle.net/2433/167635

40S subunit dissociation and proteasome-dependent RNA degradation in nonfunctional 25S rRNA decay (98 characters including spaces)

Kotaro Fujii 1,2

Makoto Kitabatake 1,2,*

Tomoko Sakata 1

Mutsuhito Ohno 1,*

1 Institute for Virus Research, Kyoto University, Kyoto 606-8507, Japan

*Correspondence: kmakoto@virus.kyoto-u.ac.jp (M.K.), hitoohno@virus.kyoto-u.ac.jp (M.O.)

2 These authors contributed equally to this work.

(Running Title) Proteasome-dependent Degradation of RNA in 25S NRD

Abstract

Eukaryotic cells have quality control systems that eliminate nonfunctional rRNAs with deleterious mutations (nonfunctional rRNA decay, NRD). We have previously reported that 25S NRD requires an E3 ubiquitin ligase complex, which is involved in ribosomal ubiquitination. However, the degradation process of nonfunctional ribosomes has remained unknown. Here, using genetic screening, we identified two ubiquitin-binding complexes, the Cdc48–Npl4–Ufd1 complex (Cdc48 complex) and the proteasome, as the factors involved in 25S NRD. We show that the nonfunctional 60S subunit is dissociated from the 40S subunit in a Cdc48-complex-dependent manner, before it is attacked by the proteasome. When we examined the nonfunctional 60S subunits that accumulated under proteasome-depleted conditions, the majority of mutant 25S rRNAs retained their full length at a single-nucleotide resolution. This indicates that the proteasome is an essential factor triggering rRNA degradation. We further showed that ribosomal ubiquitination can be stimulated solely by the suppression of the proteasome, suggesting that ubiquitin–proteasome-dependent RNA degradation occurs in broader situations, including in general rRNA turnover.

(165 words, max 175)

Introduction

Eukaryotic ribosomes are highly stable ribonucleoproteins (RNPs) composed of four rRNAs and roughly 80 ribosomal proteins. Ribosomes involve highly stable interactions between rRNAs and basic proteins (Ban et al, 2000). These static interactions contribute to the physical robustness of the ribosomes, because the stably bound proteins would hinder the access of RNases to the rRNAs (Williamson et al, 1969). As a result, the half-life of ribosomes in the mammalian liver is reported to be as long as 100 h (4 days) (Tsurugi et al, 1974). Ribosomal turnover is also only marginally observed in the growing cells of *Saccharomyces cerevisiae*. Nevertheless, some cases have been reported in which these highly stable ribosomes are rapidly degraded (Lafontaine, 2010).

One of these cases is ribophagy, a substrate-specific autophagy described in *S. cerevisiae* (Kraft et al, 2008). Both ribosomal subunits are preferentially degraded in the ribophagy pathway when cells are starved of nitrogen (Kraft et al, 2008). Ribophagy has been shown to be essential for cell survival during nutrition shortage, suggesting that the degradation of excess ribosomes may provide new building blocks to maintain cellular homeostasis. It has been reported that a deubiquitinase complex, consisting of four factors, Ubp3, Bre5, Ufd3, and Cdc48, is required for 60S ribophagy (Kraft et al, 2008; Ossareh-Nazari et al, 2010). This complex is involved in the removal of ubiquitin molecules from ribosomes, suggesting that the ubiquitination status of ribosomes is important for their degradation.

Another reported mechanism of ribosomal degradation is a quality control mechanism, nonfunctional rRNA decay (NRD), which eliminates nonfunctional 18S and 25S rRNAs (LaRiviere et al, 2006). When mutant 18S or 25S rRNAs containing a deleterious point mutation in their decoding center or peptidyltransferase center (PTC), respectively, were expressed in *S. cerevisiae*, the nonfunctional rRNAs are selectively degraded after being incorporated into the 40S and 60S particles, respectively (LaRiviere et al, 2006). Interestingly, it has been shown that 18S NRD requires the same proteins as in no-go mRNA decay (NGD) (Cole et al, 2009), which selectively eliminates aberrant mRNAs containing regions that prevent ribosomal passage (Doma & Parker, 2006), including regions with strong secondary structures, rare codons, depurination sites, etc. (Chen et al, 2010). This supports the idea that 18S NRD and NGD are different sides of the same phenomenon, both initiated by a stalled ribosome on a sense codon. It has also been shown that 25S NRD is a distinct process and requires a distinct set of factors, which are not involved in 18S NRD (Cole et al, 2009; Fujii et al, 2009).

By genetically screening a yeast knock-out collection, we have previously found that an E3 ubiquitin ligase complex containing Mms1 and Rtt101 is required for 25S NRD (Fujii et al, 2009). We have shown that ribosomal ubiquitination is induced in an Mms1–Rtt101-dependent manner when nonfunctional 25S rRNA is expressed, indicating a role for ubiquitin in this pathway (Fujii et al, 2009). However, the principle underlying the disassembly of the ribosome, a highly stable RNP, has been unclear, including whether or not the ubiquitin molecules are conjugated selectively to the nonfunctional ribosomes as a degradation tag.

In this study, we identified two ubiquitin-binding complexes, the Cdc48–Ufd1–Npl4 complex and the proteasome, as novel factors required for 25S NRD, by genetically screening the essential genes of *S. cerevisiae*. We showed that the selectively ubiquitinated nonfunctional 60S subunit dissociates from the intact 40S subunit in a Cdc48-complex-dependent manner, before it is attacked by the proteasome. We also showed that proteasome activity is essential for the initiation of 25S rRNA degradation, suggesting a role for the proteasome in removing a key factor(s) that prevents the access of RNase(s) to the ribosomes. Our results identify a previously unappreciated role of the ubiquitin–proteasome system in the degradation of stable RNAs.

Results

A novel ribosomal purification method was developed to study nonfunctional ribosomes containing a mutant 25S rRNA

We have previously reported that ubiquitin signals are enhanced in the ribosomal fractions of *S. cerevisiae* cells expressing nonfunctional mutant 25S rRNAs. This ubiquitination is dependent on an E3 ubiquitin ligase complex containing Mms1 and Rtt101, both of which are essential for 25S NRD. Although these results revealed an important role for the ubiquitin ligase in this pathway, the role of ubiquitin in the degradation process remained unclear. In this study, we investigated the principle underlying the degradation of a stable RNP, the ribosome, by identifying the direct role of ubiquitin in 25S NRD. The first question discussed in this paper is whether or not the ubiquitin molecules are conjugated specifically to the nonfunctional ribosomes.

Two other observations regarding ribosomal ubiquitination have been reported. First, the ubiquitination of Rpl28p, which constitutes the largest proportion of total ubiquitinated proteins in *S. cerevisiae*, is regulated by the cell cycle and is predominantly observed in G_1 phase (Spence et al, 2000). Second, Kraft et al. reported that nitrogen starvation stimulates ribosome-specific autophagy (ribophagy), in which the deubiquitination of the ribosomes is involved (Kraft et al, 2008). The observed ribosomal ubiquitination in 25S NRD (Fujii et al, 2009) might be a consequence of G_1 arrest or the modulation of the ribophagy pathway potentially induced by the expression of nonfunctional 25S rRNA. If either of these possibilities is true, it would

predict the general enhancement of ubiquitination in the total ribosomal pool. Another possibility is that ubiquitin molecules are selectively conjugated to nonfunctional ribosomes as tags for their degradation, as occurs in the quality control of damaged proteins. To clarify this issue, we purified nonfunctional and functional ribosomes separately to compare the extent of their ubiquitination.

To purify ribosomes containing certain mutant rRNAs, we developed an MS2 tag-based pull-down system. A sixfold (6×) repeated MS2 coat protein-binding site was inserted in a nonessential loop of 25S rRNA (Figure 1A). We observed that the expression of the MS2-tagged 25S rRNA from a polymerase II promoter, *GAL7* promoter, could rescue the growth of a polymerase I temperature-sensitive (ts) mutant (Nogi et al, 1991) on a SD–galactose plate at the restrictive temperature (Figure 1B), indicating that the 213-nt insertion in this loop did not affect the function of 25S rRNA *in vivo*. We next examined whether this tag could be used to pull down ribosomes experimentally. A glutathione S-transferase (GST)-protein-fused MS2 coat protein (GST–MS2) was coexpressed in a wild-type strain with MS2-tagged 25S rRNA. From this strain, the ribosomal fractions (60S and 80S) were prepared by sucrose density gradient sedimentation and used separately for the affinity purification of the GST fusion protein. As shown in Figure 1C, the ribosomal proteins were efficiently recovered from both the 60S and 80S fractions with this method (compare lanes 3 and 4, 7 and 8, 11 and 12) Lanes 4, 8, and 12 show the ribosomal proteins isolated from the indicated fractions by immunoprecipitation using Rpl28–Flag (Fujii et al, 2009). The recovery of the ribosomal proteins was dependent on the insertion of the MS2 tag into the 25S rRNA, and on the coexpression of the GST–MS2 protein. We confirmed that all the expected rRNAs were

observed in the isolated particles (Figure 1D and E). The introduction of a deleterious mutation in PTC, A2451U, into MS2-tagged 25S rRNA reduced the yield of ribosomes pulled down (Figure 1D and E), which is consistent with a reduction in the nonfunctional 25S rRNA by NRD in the wild-type strain. Taking these data together, we concluded that ribosomes with a certain mutation can be purified with the pull-down system developed here.

Nonfunctional ribosomes are selectively ubiquitinated

In addition to the MS2-tagged 25S rRNA described above, we also used another version of 25S rRNA that had an 18-nt insertion in the same position (Figure 1A), to express two different rRNAs in a single cell. These tagged 25S rRNAs, with or without the A2451U mutation, were coexpressed in SD–galactose medium. At mid-log phase, the medium of each culture was replaced with SD–glucose medium to shut off rRNA expression from the *GAL7* promoter. The cells were harvested at various time points and the stability of the tagged 25S rRNAs was monitored by northern blotting.

As shown in Figure 2A, we observed that nonfunctional 25S rRNAs were degraded in the wild-type strain with similar kinetics, regardless of the inserted tag sequence ("A2451U", upper panel). In contrast, both tagged 25S rRNAs were quite stable when they did not carry the A2451U mutation ("WT1", upper panel). Even when they carry the A2451U mutation, both tagged 25S rRNAs were stable in the 25S-NRD-defective strain ("*mms1*Δ", lower panel). These results indicate that the inserted tag sequences neither interfered with normal 25S NRD nor induced other types of degradation.

Therefore, we next analyzed the level of ubiquitination in ribosomes containing the MS2 tag, using GST pull-down eluates from these strains after the coexpression of the GST–MS2 protein (Figure 2B and C).

The ubiquitination was examined with Myc-tagged ubiquitin (Ellison & Hochstrasser, 1991). First, we purified the ribosomes from the strains with an Rpl28–Flag immunoprecipitation system to confirm whether ribosomal ubiquitination was also induced by the MS2-tagged mutant 25S rRNA. We observed that all the wild-type strains expressing nonfunctional 25S rRNA showed similar levels of ribosomal ubiquitination (Figure 2B, lanes 2–4). However, when only wild-type ribosomes were pulled down using the MS2 system, these signals were greatly reduced and only very faint signals were observed (Figure 2C, lane 4; we will discuss these signals later). In sharp contrast, the nonfunctional ribosomes with the A2451U mutation were highly ubiquitinated (Figure 2C, lanes 2 and 3). These observations led us to conclude that the ubiquitination observed in 25S NRD is not attributable to the universal enhancement of ubiquitination in the whole population of ribosomes. Instead, ubiquitination is highly specific to nonfunctional ribosomes, suggesting that the conjugated ubiquitin might be used as a degradation signal for nonfunctional ribosomes.

We next examined the actual role of this selective ubiquitination. To address this question, we used genetic screening to identify new factors involved in 25S NRD.

Screening for essential genes revealed the involvement of the Cdc48 complex in 25S NRD

We previously identified Mms1 and Rtt101 as factors involved in 25S NRD by screening a yeast knock-out (YKO) collection with a colony northern technique (Fujii et al, 2009). In the present study, to identify more factors, we screened another set of yeast mutants, the yeast Tet-off Hughs collection (yTHC) (Hughes et al, 2000). This collection consists of ~800 distinct mutant strains. In each strain, the promoter of a certain essential gene is replaced by the Tet-off promoter, making the strain a conditional lethal. When doxycycline (Dox) is added to the medium, it represses the expression of the essential gene, leading to the cessation of growth after several generations. We looked for a mutant strain in which the A2451U mutant rRNA is stabilized after growth is reduced by Dox treatment.

After screening several hundred strains, we noted that Cdc48 and a related factor, Ufd1, are involved in 25S NRD. The growth rates of the strains carrying these mutations decreased at 24 or 12 h after Dox was added to the medium, respectively (Figure 3A). It was indicated that the nonfunctional 25S rRNAs were stabilized in these strains (Figure 3B and C; Supplementary Figure S1A), whereas the levels of pre-rRNAs containing the PTC mutation A2451U, as well as C2452G and U2585A, persisted unchanged (Supplementary Figure S1B). The A2451U mutant 25S rRNA was degraded with normal kinetics when no Dox was added (Figure 3B and C, Dox$^-$ panel) or each repressed gene product was expressed from a plasmid (Figure 3B and C, pCDC48 or pUFD1 panel, respectively; Supplementary Figure S1C and D). These results indicate that Cdc48 and Ufd1 are newly identified factors required for 25S NRD. We also confirmed that Npl4, a binding partner of Ufd1 and Cdc48 (Meyer et al, 2000), is

involved in 25S NRD, by showing that nonfunctional mutant 25S rRNA is stabilized in an *npl4-1* ts strain (DeHoratius & Silver, 1996) at the semipermissive temperature (Figure 3D; Supplementary Figure S1E).

Recently, it has been shown that another Cdc48-containing complex, consisting of Cdc48, Ufd3, Ubp3, and Bre5, is necessary for ribophagy (Ossareh-Nazari et al., 2010). This result prompted us to examine the possibility that the same complex is also involved in 25S NRD. As shown in Supplementary Figure S2A, we initially observed that 25S NRD was inefficient to some extent in the *ufd3*Δ strain. However, in contrast to ribophagy (Ossareh-Nazari et al, 2010), the overexpression of ubiquitin rescued 25S NRD in this mutant strain (Supplementary Figure S2B). These results suggest that the observed inefficiency of 25S NRD was attributable to the effects of ubiquitin starvation, providing further proof of the requirement for ubiquitination in 25S NRD. Therefore, Ufd3 was excluded from the factors directly involved in 25S NRD. We also observed 25S NRD with normal kinetics in the *atg7*Δ strain and the *atg8*Δ strain (Supplementary Figure S2C), in which the autophagy pathway is totally absent (Tsukada and Ohsumi, 1993). Taking these data together, we concluded that 25S NRD and ribophagy are distinct processes catalyzed by distinct ubiquitin-binding complexes, which share Cdc48 as a common factor. We also confirmed that no other known binding partners of Cdc48 are required for 25S NRD (Supplementary Figure S2D).

It is well documented that the Cdc48–Ufd1–Npl4 complex is involved in the proteolysis of ubiquitinated proteins by the proteasome in divergent pathways (Ye, 2006). The proteasome might be responsible for the degradation of nonfunctional 25S rRNAs.

Therefore, we next examined this possibility.

Proteasomal activity is required for the degradation of the 25S NRD substrate

To examine the involvement of the proteasome in 25S NRD, we measured the stability of nonfunctional 25S rRNA after the cellular proteasomal activity was compromised with three different approaches (Figure 4A-C). First, we used a *cim3-1* mutant strain (Ghislain et al, 1993), which has a point mutation in Rpt6, a component of the 19S regulatory subunit of proteasome (Glickman et al, 1998). As shown in Figure 4A, the nonfunctional A2451U mutant rRNA was degraded only slowly in this mutant strain, even at the permissive temperature (upper panel). Similarly, 25S NRD was inhibited when another component of the 19S subunit, Rpt2 (Glickman et al, 1998), was depleted with the Tet-off system (Figure 4B; Supplementary Figure S2B and S3A). These instances of inhibition were rescued by a plasmid encoding the corresponding wild-type protein, Cim3/Rpt6 or Rpt2, respectively (Figure 4A and B; Supplementary Figure 3B and C). These results clearly indicate that the 19S proteasomal subunit is essential for 25S NRD.

Rpt2 and Rpt6 are two of the six AAA-ATPases in the base subcomplex of the 19S subunit (Lander et al, 2012), which are responsible for unwinding ubiquitinated proteins before their degradation by the 20S subunit (Benaroudj et al, 2001; Braun et al, 1999; Finley, 2009). To clarify whether the unwinding activity of the 19S subunit or the proteolysis by the 20S subunit is required for 25S NRD, we inhibited the proteasomal activity by treatment with MG132 using the MG132-pearmeable *erg6*Δ strain. MG132

is a potent inhibitor of the chymotrypsin-like activity of the 20S subunit (Lee & Goldberg, 1996). Figure 4C and Supplementary Figure S3D shows that the inhibition of the 20S proteasome by MG132 also interfered with the degradation of nonfunctional 25S rRNAs. The overexpression of ubiquitin did not rescue 25S NRD in this case, indicating that the inhibitory effect of MG132 on 25S NRD is not attributable to the ubiquitin starvation caused indirectly by the drug treatment (Figure 4C: Supplementary Figure S3D). Therefore, we concluded that proteolysis by the 20S proteasome is directly involved in 25S NRD. In contrast to 25S NRD, 18S NRD was not affected by the MG132 treatment (Figure 4D).

Recently, it was proposed that ubiquitin and proteasomes are also involved in ribosome biogenesis in the nucleus (Stavreva et al, 2006). To confirm that the proteasome-dependent process demonstrated here is executed in the cytoplasm, we visualized the nonfunctional 25S rRNA in several mutant strains with an in situ hybridization technique using a Cy3-labeled oligonucleotide probe (Figure 4E). Four hours after transcriptional shut-down, no signals for the nonfunctional A2451U rRNA were detected in the wild-type strain. In contrast, in the *mms1*Δ, *UFD1 tet-off*, and *RPT2 tet-off* strains, the remaining signals were distributed uniformly in the cytoplasm (Figure 4E; Supplementary Figure S3E). These observations indicate that the Cdc48 complex and the proteasome are involved in a cytoplasmic process of 25S NRD.

Considering the involvement of the Cdc48 complex and the proteasome in 25S NRD, we presumed that the observed ubiquitin molecule conjugated to the nonfunctional ribosome was a K48-linked polyubiquitin chain, a common signal for proteasomal

degradation. To confirm this, we expressed a nonfunctional mutant 25S rRNA together with Myc–ubiquitin containing either the K48R or K63R mutation and analyzed the ribosomal fractions by immunoblotting with anti-Myc antibody. The ladder-like ubiquitin signals were observed when the K63R mutant was used (Supplementary Figure S3F). In contrast, all of these signals were clearly absent when the expressed Myc–ubiquitin contained the K48R mutation, which prevents the formation of the K48-linked polyubiquitin chain. These results indicate that the ubiquitin conjugated to the nonfunctional ribosomes was the K48-linked polyubiquitin chain and supporting the conclusion that it is used as the degradation tag for the proteasome.

Ribosomal remodeling is observed in 25S NRD

To gain further insight into the details of the 25S NRD pathway, we next analyzed the size of the particles containing 25S NRD substrates in each mutant, using a sucrose density sedimentation assay. As shown in Figure 4F, Cdc48 depletion caused nonfunctional 25S rRNA to accumulate mainly in the 80S fraction, with less signal observed in the 60S fraction (panel 4). A similar pattern of accumulation was observed when Ufd1p was depleted (panel 5). In sharp contrast, when proteasomes were compromised by Rpt2 depletion, the 25S NRD substrate mainly accumulated in the 60S fraction (panel 6). Although faint signals were also detected in the 80S fraction, it is clear that the 60S/80S signal ratio in this strain was the inverse of that in strains depleted of the Cdc48 complex (Supplementary Figure S4A). The difference in the nonfunctional 25S rRNA distribution in each mutant is not attributable to the general change in the 60S/80S ratio in the cellular ribosomes, because these mutations

essentially do not affect that ratio (Supplementary Figure S4B). Instead, the different pattern of nonfunctional 25S rRNAs in Figure 4F must represent the specific effect of each mutant strain on the nonfunctional 25S rRNAs.

The observed 60S signals in the Rpt2-depleted strain do not simply represent newly synthesized unused 60S particles. Instead, these 60S signals should correspond to the degradation intermediates, which have undergone a size reduction from 80S particles. We inferred this for two reasons. First, at this time point, only signals stabilized by gene depletion or disruption were detected (Figure 4F, compare panels 3–7 with panel 2), indicating that these signals represent degradation intermediates that accumulated immediately before the steps carried out by those gene products. Second, Rpt2 depletion did not prevent nonfunctional 60S particles from forming 80S particles. When the *RPT2 tet-off mms1*Δ double mutant was used, the nonfunctional 25S rRNA signals were also observed in the 80S fraction. Essentially the same pattern was produced in the *mms1*Δ single-mutant strain (Figure 4F panel 7, compared with panel 3), suggesting that there is no significant delay in the formation of the 80S particle under Rpt2-depleted conditions. Therefore, the reduced signal in the 80S fraction and its enrichment in the 60S fraction of the Rpt2-depleted strain is attributed to the size transition from 80S to 60S of the particles containing nonfunctional 25S rRNA. This 80S to 60S size reduction is dependent on the Cdc48 complex (Figure 4F, panels 4 and 5), which functions in various pathways upstream from the proteasome (Ye, 2006).

Do the observed signals around the 60S fractions represent 60S ribosomal subunits lacking 40S subunits? Or are they incomplete 80S complexes that lack a number of

factors from both subunits? To clarify this point, we next purified and analyzed the 60S particles that accumulated in the *RPT2 tet-off* strain, using the MS2 system. As shown in Figure 5A, the accumulated 60S particles clearly retained most of the ribosomal proteins normally found in 60S subunits, when visualized by silver staining after sodium dodecyl sulfate–polyacrylamide gel electrophoresis (SDS–PAGE). We also confirmed the presence of Rpl3, 5, and 24 and the absence of Rps4 in the particles with immunoblotting (Supplementary Figure S5A). Furthermore, when the RNAs were isolated and analyzed, all the expected RNAs (25S, Figure 5B, 5.8S and 5S, Figure 5C) were detected with no apparent size reduction. Conversely, 18S rRNA was completely missing in this intermediate (Figure 5B). From these results, we conclude that nonfunctional 80S particles undergo remodeling from 80S to 60S particles with the Cdc48-dependent dissociation of the 40S subunit, before the process in which proteasomal degradation is involved.

Proteasomal degradation of key protein(s) is required for the initiation of nonfunctional 25S rRNA degradation

As shown in Figure 5B, almost full-length 25S rRNA was detected in the nonfunctional 60S subunits that accumulated in the Rpt2-depleted strain. A straightforward interpretation is that the protein degradation and RNA degradation are ordered processes; the elimination of certain protein(s) by the proteasome is required for the initiation of RNA degradation by removing key proteins that prevent the access of RNase(s) to the ribosomes. Another interpretation is that the protein degradation facilitates the processivity of unidentified exonuclease(s) by continuously removing

proteins that hinder the path of the enzyme(s). If the former is true, we should see 25S rRNA with complete ends preserved in the nonfunctional 60S particles in the Rpt2-depleted strain. Conversely, if the latter is true, degradation intermediates that lack some nucleotides or fragments at their ends should be observed. To determine which is the case, we next analyzed the accumulated nonfunctional 25S rRNAs in the Rpt2-depleted strain in detail.

When the 3′ ends of the accumulated nonfunctional 25S rRNAs were examined by northern hybridization (Figure 5D) and an RNase protection assay (Figure 5E; Supplementary Figure S5B and S7C), we found that intact 3′ ends were precisely preserved in the accumulated nonfunctional 25S rRNAs. Similarly, we confirmed by primer extension that the 5′ ends were also intact (Figure 5F and G; Supplementary Figure S7D). Based on these results, we concluded that the proteasome is required for the initiation of 25S rRNA degradation in NRD, but not for the processivity of the RNase(s).

Ribosomes are continuously degraded by the ubiquitin–proteasome system

Is the ubiquitin–proteasome-assisted degradation of ribosomal particles described in this paper limited to 25S NRD? Or is it observed in other, more general cases of ribosomal degradation? To address this question, we next evaluated whether ribosomal ubiquitination is enhanced when ribosomal degradation is artificially induced by drug treatments.

It has been reported that the extensive decay of rRNAs can be artificially induced by the treatment of yeast cells with several compounds, including H_2O_2, acetic acid, and methylmethanesulfonate (Supplementary Figure S6A) (Mroczek & Kufel, 2008; Thompson et al, 2008). We added these drugs to the cultures to induce rRNA decay. During the lag period before rRNA degradation, we immunopurified the ribosomes using Rpl28–Flag and analyzed the ubiquitination status of those ribosomes using a Myc–ubiquitin system (Figure 6A and B; Supplementary Figure S6B). In all the cases examined, ribosomal ubiquitination was enhanced by the drug treatment in a dose-dependent manner. The distribution of the ubiquitination signals shifted to higher molecular weights. The total intensity of the signals also increased. These results clearly show that ribosomal ubiquitination occurs when ribosomal degradation is triggered by chemical stressors. The ubiquitination described here was also observed in the *mms1*Δ strain (Figure 6A, lanes 7-10), suggesting that multiple ubiquitin ligases are involved in the ubiquitination of the damaged ribosomes.

Interestingly, during these experiments, we noticed that ribosomes from untreated cells always displayed some level of ubiquitination signal (Figure 6A, lanes 1 and 7; see also Figure 2B, lane 1). These faint signals were also observed in MS2-purified wild-type ribosomes (Figure 2C, lanes 1, 4, and 5). We hypothesized that ribosomes might be slowly degraded by the ubiquitin–proteasome system, even in normally growing cells. If this is the case, ribosomal ubiquitination will be enhanced without drug treatments when proteasomal activity is compromised. To investigate this possibility, we examined whether Rpt2 depletion influenced the ubiquitination status of the ribosomes.

As shown in Figure 6C, Rpt2p depletion markedly elevated the ubiquitination of the 60S ribosomal subunit (compare lane 5 with lanes 6 and 7). In this assay, the Rpl28–Flag-containing complex was immunopurified from the 60S fraction prepared from the *RPT2 tet-off* strain expressing Rpl28–Flag and Myc–Ubi (Supplementary Figure S6C), and ubiquitination was detected with anti-Myc antibody after SDS–PAGE. When Rpl28–Flag and Myc–Ubi were expressed separately in different strains and the 60S fractions from those strains were mixed and used for immunoprecipitation, almost no ubiquitination signals were recovered (lane 8), showing that the ubiquitinated proteins in lanes 6 and 7 are ribosomal proteins or proteins physiologically associated with the ribosomes. These results suggest that cellular ribosomes are more or less continuously ubiquitinated and degraded, even in normally growing cells. A similar result was obtained when 40S subunits were analyzed (Figure 6D, compare lane 5 with lanes 6 and 7). Therefore, we conclude that the degradation of stable RNPs by the ubiquitin–proteasome system is not specific to 25S NRD but occurs more widely, as ribosomal ubiquitination is observed in the degradation of drug-treated ribosomes and the natural turnover of normally growing cells.

Discussion

In this study, we have shown that the Cdc48–Ufd1–Npl4 complex and the proteasome are the essential factors involved in the late steps of 25S NRD. The 40S subunit dissociated from the nonfunctional 60S subunit in a Cdc48-complex-dependent manner. The affinity purification of nonfunctional 60S particles that accumulated in a proteasome-depleted strain indicated that the proteasome is required for the initiation of rRNA degradation in 25S NRD. Moreover, we have provided evidence that the ubiquitin–proteasome system is involved in stress induced ribosomal degradation and ribosomal turnover.

Novel affinity purification system for eukaryotic ribosomes containing a certain mutation

We have described here a newly developed affinity purification method for ribosomes. Using this system, ribosomes with a certain mutation in their 25S rRNA were biochemically isolated. To date, there have been a number of reports characterizing eukaryotic ribosomes containing mutant 25S rRNAs (Macbeth & Wool, 1999; Panopoulos et al, 2004; Rakauskaite & Dinman, 2008). However, in those studies, entire populations of cellular ribosomes were replaced by the mutant ribosome to be characterized. This limits the variety of mutants than can be characterized, because nonfunctional ribosomes with a critical mutation cannot be prepared with this approach. With the MS2-based purification method described here, any mutant ribosomes containing a deleterious mutation(s) in the 25S rRNA can be isolated, because the

growth of the cells is supported by cellular ribosomes in this case. This offers a new avenue for the biochemical characterizations of eukaryotic ribosomes. X-ray crystallography has recently begun to reveal the detailed structures of these ribosomes at atomic resolution (Ben-Shem et al, 2010; Rabl et al, 2011).

Role of the Cdc48 complex in the disassembly of ribosomes

We have shown that the depletion of the Cdc48–Npl4–Ufd1 complex causes nonfunctional 25S rRNAs to accumulate in the 80S particle. When a downstream step was interrupted by proteasomal depletion, those nonfunctional 25S rRNAs were detected in the 60S subunit. These results indicate that the Cdc48 complex is essential for the segregation of the 40S subunit from the nonfunctional 60S subunit. The dissociated 40S subunit will probably be reused for the next round of translation, because the dissociated 40S subunit should be intact, and recycling the 40S particle will reduce cellular energy consumption during the reconstruction of the massive ribosome particle.

An interesting possibility is that the Cdc48 complex directly catalyzes this segregation. Cdc48 belongs to the AAA-ATPase family (Ogura & Wilkinson, 2001). It has been reported that the Cdc48–Npl4–Ufd1 complex is involved in the segregation of misfolded proteins from the ER to the cytoplasm during ERAD (Ye et al, 2001). In general, the heterodimer Npl4p–Ufd1p directly binds ubiquitin (Meyer et al, 2002), and the mechanical force for the segregation is provided by a hexamer of Cdc48p (Rape et al, 2001; Ye et al, 2001). Using the ubiquitinated protein on the 60S subunit as a handle,

this complex might physically dissociate the 40S subunit from the nonfunctional 80S particle. Another possibility is that the Cdc48 complex indirectly assists the function of other factor(s) involved in subunit dissociation (Kurata et al, 2010; Pisarev et al, 2010; Shoemaker et al, 2010). An *in vitro* reconstitution system for Cdc48–Npl4–Ufd1 activity (Shcherbik & Haines, 2007) would effectively address this issue.

Use of a variety of RNP degradation mechanisms

It has recently been shown that the RNA helicase Upf1 is involved in the disassembly of mRNPs in nonsense-mediated mRNA decay (Franks et al, 2010). Using RNA helicase for the disassembly of relatively unstable mRNPs is reasonable, because such disassembly occurs quite often and RNA-binding proteins can be recycled in this situation (Bono & Gehring, 2011). A similar mechanism is also observed in the degradation of the intron lariat complex, where the RNA helicase Prp43 is involved in the disassembly (Arenas & Abelson, 1997; Tsai et al, 2005; Yoshimoto et al, 2009). In contrast, we have shown in this study that the disassembly of a stable RNP, the 60S ribosomal subunit, is processed by a distinct mechanism, a proteasomal degradation dictated by the specific ubiquitination of nonfunctional ribosomes (Figure 7). Why do cells not recycle proteins after the disassembly of stable RNPs?

There seem to be at least two reasons. First, we infer that it is because recycling ribosomal proteins would be risky for cells. Most of the ribosomal proteins are highly basic and chemically likely to aggregate with cellular RNAs (Jakel et al, 2002). Ribosomal protein(s) should be degraded before RNA degradation to avoid the potential

risk of harmful ribosomal proteins dispersed in the cytoplasm. Second, it could be because the ribosomes are composed of a number of components. Most ribosomal proteins and the entire sequences of rRNAs are well conserved, from yeasts to humans (Lecompte et al, 2002), implying that any change in these conserved components might harm the ribosomal function. The identification of the aberrant component in a large nonfunctional ribosome might cost more than the degradation and reconstruction of the total complex, when we consider that cellular stress must randomly induce various ribosomal damage to each component. One such stress is the oxidative stress examined in Figure 6A. In this case, as was shown, various types of ribosomal ubiquitination were induced, suggesting that multiple components were damaged by this treatment.

We have shown in this study that the ubiquitination of ribosomes (both the 60S and 40S subunits) occurs in various situation in which ribosomes are degraded, except in 18S NRD (Figure 4D). How far can we apply this principle of RNP degradation to other stable RNPs? There are a number of stable RNPs in eukaryotic cells. These stable RNPs must also eventually be degraded, for various reasons, including quality control and changes in the RNPs' repertoires during differentiation, apoptosis, etc. It will be very interesting to clarify whether ubiquitin–proteasome-directed RNP disassembly is also involved in the degradation of these stable RNPs.

Methods

Plasmids, yeast strains, and growth conditions

Please see the Supplemental Experimental Procedures.

RNA purification and analysis

To extract the total RNA from yeast cells, we used the MasterPure™ Yeast RNA Purification Kit (Epicentre Biotechnologies). Sepasol-RNA1 Super (Nacalai Tesque) was used to extract the RNA from cell lysates or purified ribosomes. In a northern analysis of the stability of the tagged rRNAs, 500 ng of total RNA was loaded into the lane at time 0. The amount of RNA loaded into the other lanes was increased according to the growth of the cells, measured as the absorbance at 600 nm (A_{600}), leaving the signals of the stable RNA species unchanged.

RNase H digestion was performed with 1.5 μg of total RNA and 0.25 μM oligonucleotide DNA (Kota031), according to Uyeno et al (Uyeno et al, 2004). Complete digestion produced a ~220-nt fragment containing the 5′ end of the 18-nt-tagged 25S rRNAs and a ~440-nt fragment of the MS2-tagged RNAs.

Ribosome purification and immunoblotting

The purification of total ribosomes using the Flag-tagged ribosomal protein Rpl28 has been described elsewhere (Fujii et al, 2009). To isolate the ribosomes containing plasmid-derived rRNAs, MS2-tagged 25S rRNA and GST–MS2 were coexpressed. Approximately 800 A_{600} units cells were harvested and disrupted in liquid nitrogen in a mortar (Inada et al, 2002). The lysate was dissolved in 1 mL IPP150 (10 mM Tris-HCl

[pH 8.0], 150 mM NaCl, 2.5 mM $MgCl_2$, 0.1% NP-40) supplemented with Complete Protease Inhibitor Cocktail (Roche) and 20 mM N-ethylmaleimide. The ribosomes containing MS2-tagged rRNA and GST–MS2 were pulled down with glutathione Sepharose beads from the 60S and 80S fractions of a sucrose density gradient. The ribosomes were recovered after elution with 100 mM reduced glutathione. To immunoblot the ubiquitinated ribosomes, equal amounts of ribosomes in the eluates were subjected to 5%–20% gradient SDS–PAGE and transferred to a nitrocellulose membrane with a semidry blotting apparatus. To analyze the cosedimented proteins, the proteins were visualized by silver staining after 10%–20% gradient SDS–PAGE.

In situ hybridization

All the cells were grown in SD–raffinose to A_{600} = 0.5. The medium was then replaced with SD–galactose to induce the expression of the tagged rRNAs from the *GAL7* promoter. Six hours after induction, the medium was replaced again with SD–glucose to shut-off transcription. The cells were harvested onto a glass slide and analyzed 4 h after transcriptional shut-off. The specimens were prepared as described elsewhere (Fujii et al, 2009). Microscopic analyses were performed using Olympus BX61 and UAPON 150XO microscopes (NA = 1.45). A series of 15~20 Z-stuck was captured for each picture and processed with AutoQuant deconvolution using MetaMorph. The best-focused picture for each specimen was selected and presented.

RNase protection assay and primer extension

An RNase protection assay was performed using an RNase cocktail (Ambion). The template RNAs (10 ng) and probes (1×10^4 cpm) were hybridized overnight at 45 °C in 1

× hybridization buffer (40 mM PIPES [pH 6.8], 1 mM EDTA [pH 8.0], 0.4 mM NaCl, 80% formamide). The RNase digestion mixture (300 mM NaCl, 10 mM Tris-HCl [pH 7.4], 5 mM EDTA, 0.5 U/μL RNase A, 20 U/μL RNase T1) was added to digest the single-stranded RNAs in the reaction. After the reaction was incubated at 30 °C for 60 min, the RNases were inactivated by the addition of sodium dodecyl sulfate and proteinase K. The RNase-resistant hybrids were then analyzed by gel electrophoresis and autoradiography (Sambrook, 2001). The probe used in this study was synthesized *in vitro* with T7 RNA polymerase (Promega). The PCR product generated with primers Kota379 and Kota383 was used as the template. This probe contains a 150-nt region complementary to the 3′ end of 25S rRNA and overhangs both the 5′ end (30-nt) and 3′ end (8-nt). The control RNA used to indicate the 3′ end of the mature 25S rRNA was also transcribed *in vitro* with the T7 RNA polymerase system, using the Kota381–Kota382 PCR product as the template. For primer extension, 0.5 μg of the purified RNAs and 0.25 pmol of ^{32}P-labeled primer were mixed and treated with reverse transcriptase (ReverTra Ace, Toyobo), following the manufacturer's instructions. The reaction was then analyzed by autoradiography after separation on an 8% acrylamide gel containing 7 M urea.

Analysis of the ubiquitination of 40S and 60S ribosomal particles in the *RPT2 tet-off* strain

To purify 40S and 60S ribosomal particles, Rps2–Flag and Rpl28–Flag were expressed, respectively. The *RPT2 tet-off* strain expressing Myc–Ubi was grown in SD–glucose. When the cells reached A_{600} = 0.5, they were diluted in the same medium containing 10 μg/mL Dox, to maintain the log phase for the indicated times. Approximately 500 A_{600}

units cells were harvested and disrupted in liquid nitrogen in a mortar (Inada et al, 2002). The lysate was fractionated on a sucrose density gradient containing 40 mM EDTA and the 40S and 60S fractions were collected. The ribosomal particles from the *RPT2 tet-off* strain were immunoprecipitated with anti-Flag agarose and washed with IPP150 (10 mM Tris-HCl [pH 8.0], 150 mM NaCl, 2.5 mM $MgCl_2$, 0.1% NP-40). To elute the ribosomes, IPP150 was used with 3× Flag peptides (Sigma) at a concentration of 0.25 mg/mL. Before pull-down, the untagged wild-type 40S and 60S fractions were mixed with the *RPT2 tet-off* strain-derived 40S and 60S fractions, respectively. To evaluate the nonspecific binding of ubiquitinated peptides to ribosomes, as a control, the Flag-tagged ribosomal particles from the wild-type strain were immunopurified after 40S or 60S fractions from RPT2 tet-off cells, without Flag tag expression, were mixed. The purified ribosomes were separated by 5%–20% SDS–PAGE and the ubiquitinated proteins were detected with an anti-Myc polyclonal antibody.

Acknowledgments

We thank Dr Pamela A. Silver for generously providing the yeast strain, Dr Kaori Shinmyouzu and Dr Akira Nakamura for the mass-spectrometric analysis, and Dr Hideji Yoshida for technical advice and discussions. We also thank Tokie Sakai and Kodai Sano for their technical assistance. This work was supported by PRESTO, JST, in a grant to M.K., and a Grant-in-Aid for Scientific Research on Innovative Areas “RNA regulation” (no. 20112006) from the Ministry of Education, Culture, Sports, Science and Technology of Japan to M.K. and M.O. K.F. and T.S. are Japan Society for the Promotion of Science Research Fellows.

Supplementary information is available at EMBO Journal Online.

Figure Legends

Figure 1

Ribosomes containing MS2-tagged rRNAs can be affinity purified with GST–MS2

(A) Schematic representation of the plasmids used for rRNA expression. An 18-nt tag or MS2 tag was inserted into the 5′ region of the 25S rRNA. Both rRNAs were transcribed from the *GAL7* promoter by RNA polymerase II.

(B) Complementation test of a RNA polymerase I temperature-sensitive (ts) strain. The NOY401 strain containing various plasmids were grown and spotted onto SD–galactose plates after a series of 10-fold dilutions.

(C–E) Protein and RNA compositions of affinity-purified ribosomes. (C) Each ribosomal fraction was isolated by sucrose density gradient sedimentation from the strain expressing the indicated plasmids and subjected to GST pull-down. The proteins were visualized by silver staining. Lanes 4, 8, and 12 show the intact ribosomal particles immunopurified with Rpl28–Flag from the fractions. GST–MS2cp: GST–MS2 coat protein. (D, E) RNAs were separated on the indicated gels and visualized with SYBR Gold staining.

Figure 2

Nonfunctional ribosomes are selectively ubiquitinated and degraded in an Mms1-dependent manner

(A) Northern blotting of 18-nt- or MS2-tagged 25S rRNAs. The total RNAs were isolated from cells carrying the indicated plasmids after transcriptional shut-off. These RNAs were cleaved with RNase H (Supplementary Figure S7A). Northern hybridization was

performed using a probe that detected both tagged RNAs.

(B, C) Immunoblotting of ribosomes purified from cells expressing the indicated tagged rRNAs and Myc–ubiquitin. (B) Ribosomes were Rpl28–Flag immunopurified. In lane 6, an empty vector was used instead of pMyc–Ubi. In lane 7, a wild-type strain with untagged Rpl28 was used. (C) GST–MS2 affinity purification of the ribosomal fraction sedimented by sucrose density gradient centrifugation. In lane 6, an 18-nt-tagged wild-type rRNA was expressed as the negative control.

Figure 3

Nonfunctional 25S rRNAs were stabilized in Cdc48-complex-deficient strains

(A) Growth curves for *CDC48* and *UFD1 tet-off* strains in the presence (Dox^+) and absence (Dox^-) of Dox. The cells were grown in SD–galactose medium and A_{600} was monitored at the indicated times. The arrows indicate the time points at which the cells were harvested for the following analyses.

(B,C) Time course experiments to test the stability of 25S rRNA in *CDC48 tet-off* (B) and *UFD1 tet-off* (C) strains. After Dox treatment, the stability of the 18-nt-tagged 25S rRNA was monitored by northern blotting. The pCDC48 plasmid or pUFD1 plasmid was cointroduced into the tet-off strains, as indicated.

(D) Stability of nonfunctional 25S rRNA in an *npl4-1* mutant strain. The *npl4-1* ts strain was grown at the indicated temperature. The pNPL4 plasmid was cointroduced into the strain as indicated.

Figure 4

Proteasome activity is required for 25S NRD

(A–D) Stability of nonfunctional rRNA in a proteasome-inhibited cell. (A–C) The 18-nt-tagged 25S rRNA was detected by northern blotting. (A) The *cim3-1* ts strain was grown at the permissive temperature. (B) Proteasomes were depleted in the *RPT2 tet-off* strain with Dox treatment for 12 h. (C, D) MG132 was administered at the indicated concentrations to the *erg6*Δ strain containing the combination of plasmids indicated, to overexpress ubiquitin. (D) The other 16-nt-tagged 18S rRNAs, with or without A1492C mutation, were detected by northern blotting.

(E, F) Subcellular localization of 18-nt-tagged 25S rRNAs in various mutant strains. After transcriptional shut-off, the cells were harvested at the indicated time points. (E) The tagged 25S rRNAs were visualized with an in situ hybridization technique. Scale bar, 4 μm. (F) Cleared lysates were resolved on a 10%–40% sucrose gradient and the amounts of tagged rRNA were visualized by northern blotting.

Figure 5

Nonfunctional 60S particles that accumulated under proteasome-depleted conditions contained most ribosomal proteins and complete sets of all three rRNAs

(A–G) The protein and RNA compositions of nonfunctional ribosomes affinity purified with GST–MS2 from the *RPT2 tet-off* strain 4 h after transcriptional shut-off. GST pull-down was performed using ~60S fractions. (A) The eluates were separated and silver stained. In lane 3, WT1–MS2-containing 60S ribosomal particles were purified from the wild-type strain (*nonribosomal proteins). (B, C) Purified RNAs were separated and stained with SYBR Gold. In lanes 2 and 4, total RNA was purified from the wild-type strain. (D) Northern hybridization was performed using a prove which was designed to bind the 3′-most region of 25S rRNA (position +3251). The number

below each lane shows the relative signal intensity. (E) An RNase protection assay was used to examine the 3′ ends of the 25S rRNAs. In lanes 5 and 6, the 3′ region of the 25S rRNA was transcribed *in vitro* and used. For lanes 7–9, total RNAs diluted two-fold were used. For lane 10, no target RNA was added to the reaction. Lane 11 is the no-RNase control. (F, G) Primer extension showed the 5′ ends of the 25S rRNAs. The primer used was designed to bind the region into which the tags were inserted (Supplementary Figure S7D). (G) The corresponding sequence for the sense strand of the 25S rDNA is shown. The 5′ end of the mature 25S rRNA is indicated by an arrowhead.

Figure 6

Ribosomes are continuously ubiquitinated and degraded by proteasomes

(A, B) Ubiquitination signals induced by stress. (A) Wild-type and *mms1*Δ cells were grown in SD–glucose medium and treated for 2 h with 0, 0.25, 0.5, and 1 mM H_2O_2. In lane 5, an empty vector was used instead of pMyc–Ubi. In lane 6, another empty vector was used instead of pRpl28–Flag. (B) Wild-type cells were treated with acetic acid at a final concentration of 90 mM. Ribosomes were isolated at the indicated time points.

(C) Ubiquitinated 60S ribosomal particles accumulated under Rpt2p-depleted conditions. The *RPT2 tet-off* strain was treated for the indicated times with 10 μg/mL Dox. The 60S ribosomal fractions were collected by 10%–40% sucrose gradient sedimentation containing 40 mM EDTA. The 60S particles from the *RPT2 tet-off* strain were immunoprecipitated (lanes 5–7). Before the pull-down assay, untagged wild-type 60S fractions were mixed with the *RPT2-tet-off* strain-derived 60S fractions. To evaluate the nonspecific binding of ubiquitinated proteins to ribosomes, as a control,

60S particles from the wild-type strain were immunopurified after they were mixed with the 60S fraction from RPT2 tet-off cells (lane 8). The ubiquitinated proteins in the mixture of 60S fractions are shown in lanes 1–4.

(D) Ubiquitinated 40S ribosomal particles under Rpt2-depleted conditions. A similar set of experiments to (C) was performed using the 40S fractions and Rps2–Flag.

Figure 7

A model of RNP degradation

In mRNP degradation, mRNPs are disassembled by RNA helicases (Upf1 in NMD). This RNP disassembly step is essential for mRNA degradation by RNases. During ribosomal degradation, E3 ubiquitin ligase first ubiquitinates the ribosomal proteins. Using these ubiquitins as tags, the Cdc48 complex promotes the dissociation of the 40S subunit. The proteasome degrades key protein(s) from the 60S particles and then triggers the initiation of RNA decay.

References

Arenas JE, Abelson JN (1997) Prp43: An RNA helicase-like factor involved in spliceosome disassembly. *Proc Natl Acad Sci U S A* **94:** 11798-11802

Ban N, Nissen P, Hansen J, Moore PB, Steitz TA (2000) The complete atomic structure of the large ribosomal subunit at 2.4 A resolution. *Science* **289:** 905-920

Ben-Shem A, Jenner L, Yusupova G, Yusupov M (2010) Crystal structure of the eukaryotic ribosome. *Science* **330:** 1203-1209

Benaroudj N, Tarcsa E, Cascio P, Goldberg AL (2001) The unfolding of substrates and ubiquitin-independent protein degradation by proteasomes. *Biochimie* **83:** 311-318

Bono F, Gehring NH (2011) Assembly, disassembly and recycling: the dynamics of exon junction complexes. *RNA Biol* **8:** 24-29

Braun BC, Glickman M, Kraft R, Dahlmann B, Kloetzel PM, Finley D, Schmidt M (1999) The base of the proteasome regulatory particle exhibits chaperone-like activity. *Nature cell biology* **1:** 221-226

Chen L, Muhlrad D, Hauryliuk V, Cheng Z, Lim MK, Shyp V, Parker R, Song H (2010) Structure of the Dom34-Hbs1 complex and implications for no-go decay. *Nat Struct Mol Biol* **17:** 1233-1240

Cole SE, LaRiviere FJ, Merrikh CN, Moore MJ (2009) A convergence of rRNA and mRNA quality control pathways revealed by mechanistic analysis of nonfunctional rRNA decay. *Mol Cell* **34:** 440-450

DeHoratius C, Silver PA (1996) Nuclear transport defects and nuclear envelope alterations are associated with mutation of the Saccharomyces cerevisiae NPL4 gene. *Mol Biol Cell* **7:** 1835-1855

Doma MK, Parker R (2006) Endonucleolytic cleavage of eukaryotic mRNAs with stalls in translation elongation. *Nature* **440:** 561-564

Ellison MJ, Hochstrasser M (1991) Epitope-tagged ubiquitin. A new probe for analyzing ubiquitin function. *The Journal of biological chemistry* **266:** 21150-21157

Finley D (2009) Recognition and processing of ubiquitin-protein conjugates by the proteasome. *Annu Rev Biochem* **78:** 477-513

Franks TM, Singh G, Lykke-Andersen J (2010) Upf1 ATPase-dependent mRNP disassembly is required for completion of nonsense- mediated mRNA decay. *Cell* **143:** 938-950

Fujii K, Kitabatake M, Sakata T, Miyata A, Ohno M (2009) A role for ubiquitin in the clearance of nonfunctional rRNAs. *Genes Dev* **23:** 963-974

Ghislain M, Udvardy A, Mann C (1993) S. cerevisiae 26S protease mutants arrest cell division in G2/metaphase. *Nature* **366:** 358-362

Glickman MH, Rubin DM, Coux O, Wefes I, Pfeifer G, Cjeka Z, Baumeister W, Fried VA, Finley D (1998) A subcomplex of the proteasome regulatory particle required for ubiquitin-conjugate degradation and related to the COP9-signalosome and eIF3. *Cell* **94:**

615-623

Hughes TR, Marton MJ, Jones AR, Roberts CJ, Stoughton R, Armour CD, Bennett HA, Coffey E, Dai H, He YD, Kidd MJ, King AM, Meyer MR, Slade D, Lum PY, Stepaniants SB, Shoemaker DD, Gachotte D, Chakraburtty K, Simon J, Bard M, Friend SH (2000) Functional discovery via a compendium of expression profiles. *Cell* **102:** 109-126

Inada T, Winstall E, Tarun SZ, Jr., Yates JR, 3rd, Schieltz D, Sachs AB (2002) One-step affinity purification of the yeast ribosome and its associated proteins and mRNAs. *RNA* **8:** 948-958

Jakel S, Mingot JM, Schwarzmaier P, Hartmann E, Gorlich D (2002) Importins fulfil a dual function as nuclear import receptors and cytoplasmic chaperones for exposed basic domains. *EMBO J* **21:** 377-386

Kraft C, Deplazes A, Sohrmann M, Peter M (2008) Mature ribosomes are selectively degraded upon starvation by an autophagy pathway requiring the Ubp3p/Bre5p ubiquitin protease. *Nat Cell Biol* **10:** 602-610

Kurata S, Nielsen KH, Mitchell SF, Lorsch JR, Kaji A, Kaji H (2010) Ribosome recycling step in yeast cytoplasmic protein synthesis is catalyzed by eEF3 and ATP. *Proc Natl Acad Sci U S A* **107:** 10854-10859

Lafontaine DL (2010) A 'garbage can' for ribosomes: how eukaryotes degrade their ribosomes. *Trends Biochem Sci* **35:** 267-277

Lander GC, Estrin E, Matyskiela ME, Bashore C, Nogales E, Martin A (2012) Complete subunit architecture of the proteasome regulatory particle. *Nature* **482:** 186-191

LaRiviere FJ, Cole SE, Ferullo DJ, Moore MJ (2006) A late-acting quality control process for mature eukaryotic rRNAs. *Mol Cell* **24:** 619-626

Lecompte O, Ripp R, Thierry JC, Moras D, Poch O (2002) Comparative analysis of ribosomal proteins in complete genomes: an example of reductive evolution at the domain scale. *Nucleic acids research* **30:** 5382-5390

Lee DH, Goldberg AL (1996) Selective inhibitors of the proteasome-dependent and vacuolar pathways of protein degradation in Saccharomyces cerevisiae. *J Biol Chem* **271:** 27280-27284

Macbeth MR, Wool IG (1999) Characterization of in vitro and in vivo mutations in non-conserved nucleotides in the ribosomal RNA recognition domain for the ribotoxins ricin and sarcin and the translation elongation factors. *Journal of molecular biology* **285:** 567-580

Meyer HH, Shorter JG, Seemann J, Pappin D, Warren G (2000) A complex of mammalian ufd1 and npl4 links the AAA-ATPase, p97, to ubiquitin and nuclear transport pathways. *The EMBO journal* **19:** 2181-2192

Meyer HH, Wang Y, Warren G (2002) Direct binding of ubiquitin conjugates by the mammalian p97 adaptor complexes, p47 and Ufd1-Npl4. *The EMBO journal* **21:** 5645-5652

Mroczek S, Kufel J (2008) Apoptotic signals induce specific degradation of ribosomal RNA in yeast. *Nucleic Acids Res* **36:** 2874-2888

Nogi Y, Yano R, Nomura M (1991) Synthesis of large rRNAs by RNA polymerase II in mutants of Saccharomyces cerevisiae defective in RNA polymerase I. *Proc Natl Acad Sci U S A* **88:** 3962-3966

Ogura T, Wilkinson AJ (2001) AAA+ superfamily ATPases: common structure--diverse function. *Genes Cells* **6:** 575-597

Ossareh-Nazari B, Bonizec M, Cohen M, Dokudovskaya S, Delalande F, Schaeffer C, Van Dorsselaer A, Dargemont C (2010) Cdc48 and Ufd3, new partners of the ubiquitin protease Ubp3, are required for ribophagy. *EMBO Rep* **11:** 548-554

Panopoulos P, Dresios J, Synetos D (2004) Biochemical evidence of translational infidelity and decreased peptidyltransferase activity by a sarcin/ricin domain mutation of yeast 25S rRNA. *Nucleic acids research* **32:** 5398-5408

Pisarev AV, Skabkin MA, Pisareva VP, Skabkina OV, Rakotondrafara AM, Hentze MW, Hellen CU, Pestova TV (2010) The role of ABCE1 in eukaryotic posttermination ribosomal recycling. *Mol Cell* **37:** 196-210

Rabl J, Leibundgut M, Ataide SF, Haag A, Ban N (2011) Crystal structure of the eukaryotic 40S ribosomal subunit in complex with initiation factor 1. *Science* **331:** 730-736

Rakauskaite R, Dinman JD (2008) rRNA mutants in the yeast peptidyltransferase center reveal allosteric information networks and mechanisms of drug resistance. *Nucleic Acids Res* **36:** 1497-1507

Rape M, Hoppe T, Gorr I, Kalocay M, Richly H, Jentsch S (2001) Mobilization of processed, membrane-tethered SPT23 transcription factor by CDC48(UFD1/NPL4), a ubiquitin-selective chaperone. *Cell* **107:** 667-677

Sambrook J (2001) *Molecular cloning : a laboratory manual / Joseph Sambrook, David W. Russell,* Cold Spring Harbor, N.Y. :: Cold Spring Harbor Laboratory.

Shcherbik N, Haines DS (2007) Cdc48p(Npl4p/Ufd1p) binds and segregates membrane-anchored/tethered complexes via a polyubiquitin signal present on the anchors. *Mol Cell* **25:** 385-397

Shoemaker CJ, Eyler DE, Green R (2010) Dom34:Hbs1 promotes subunit dissociation and peptidyl-tRNA drop-off to initiate no-go decay. *Science* **330:** 369-372

Spence J, Gali RR, Dittmar G, Sherman F, Karin M, Finley D (2000) Cell cycle-regulated modification of the ribosome by a variant multiubiquitin chain. *Cell* **102:** 67-76

Stavreva DA, Kawasaki M, Dundr M, Koberna K, Muller WG, Tsujimura-Takahashi T, Komatsu W, Hayano T, Isobe T, Raska I, Misteli T, Takahashi N, McNally JG (2006) Potential roles for ubiquitin and the proteasome during ribosome biogenesis. *Mol Cell Biol* **26:** 5131-5145

Thompson DM, Lu C, Green PJ, Parker R (2008) tRNA cleavage is a conserved response to oxidative stress in eukaryotes. *RNA* **14:** 2095-2103

Tsai RT, Fu RH, Yeh FL, Tseng CK, Lin YC, Huang YH, Cheng SC (2005) Spliceosome disassembly catalyzed by Prp43 and its associated components Ntr1 and Ntr2. *Genes & development* **19:** 2991-3003

Tsurugi K, Morita T, Ogata K (1974) Mode of degradation of ribosomes in regenerating rat liver in vivo. *Eur J Biochem* **45:** 119-126

Uyeno Y, Sekiguchi Y, Sunaga A, Yoshida H, Kamagata Y (2004) Sequence-specific cleavage of small-subunit (SSU) rRNA with oligonucleotides and RNase H: a rapid and simple approach to SSU rRNA-based quantitative detection of microorganisms. *Appl Environ Microbiol* **70:** 3650-3663

Williamson R, Lanyon G, Paul J (1969) Preferential degradation of "messenger RNA" in reticulocytes by ribonuclease treatment and sonication of polysomes. *Nature* **223:** 628-630

Ye Y (2006) Diverse functions with a common regulator: ubiquitin takes command of an AAA ATPase. *J Struct Biol* **156:** 29-40

Ye Y, Meyer HH, Rapoport TA (2001) The AAA ATPase Cdc48/p97 and its partners transport proteins from the ER into the cytosol. *Nature* **414:** 652-656

Yoshimoto R, Kataoka N, Okawa K, Ohno M (2009) Isolation and characterization of post-splicing lariat-intron complexes. *Nucleic Acids Res* **37:** 891-902

Figure 1 (Kitabatake)

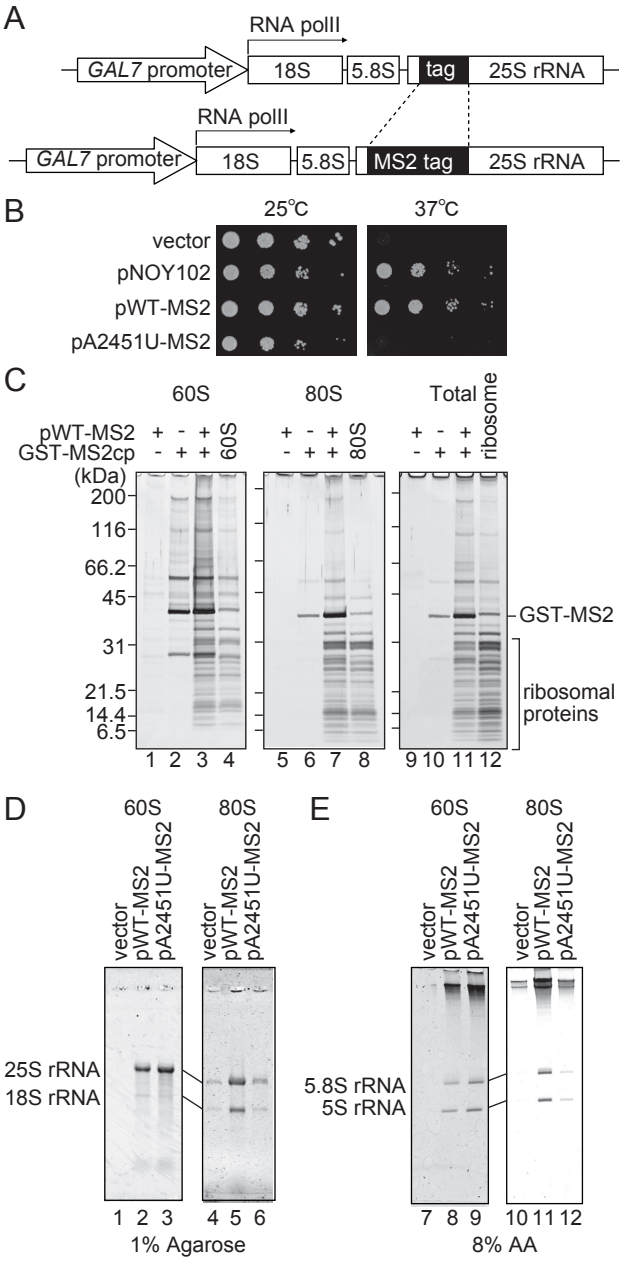

Figure 2 (Kitabatake)

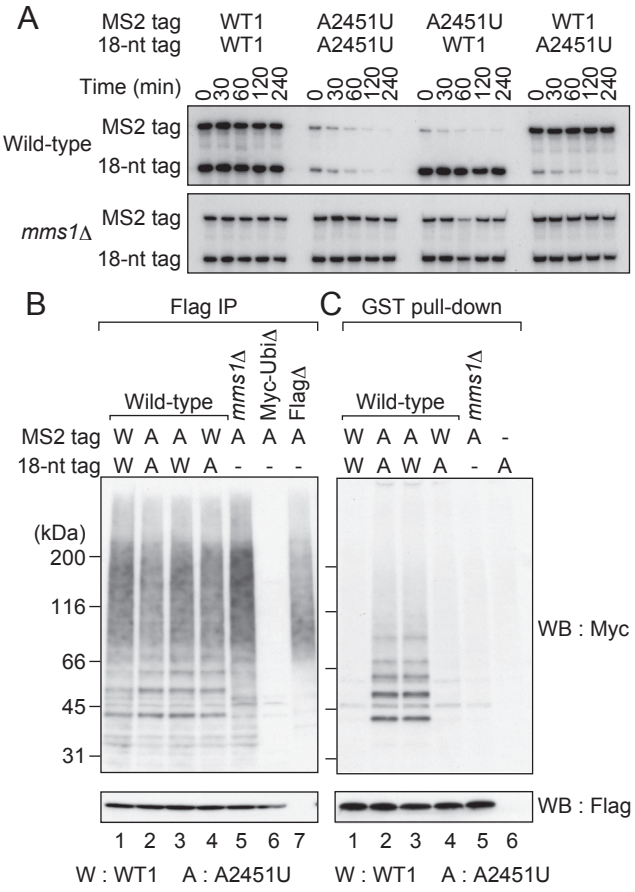

Figure 3 (Kitabatake)

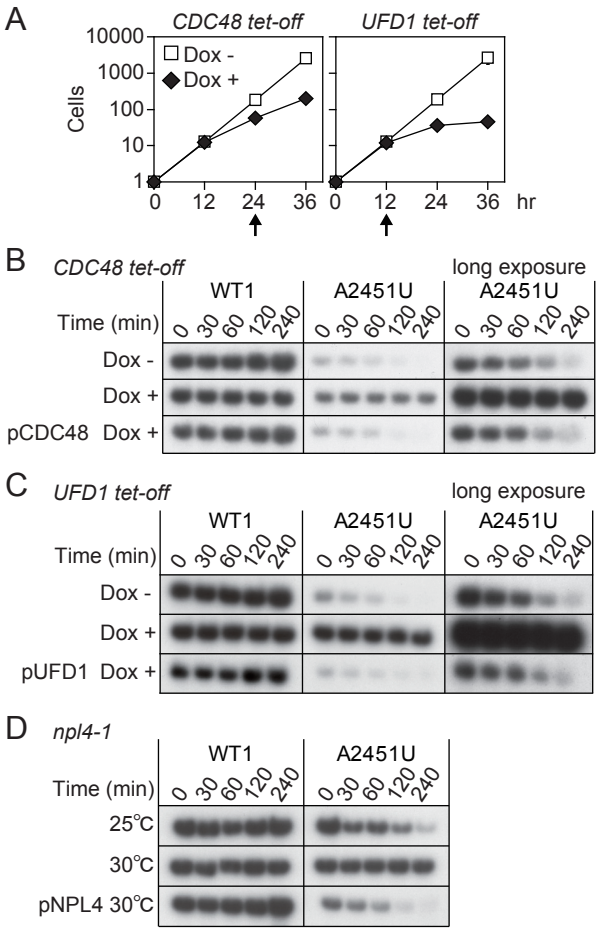

Figure 4 (Kitabatake)

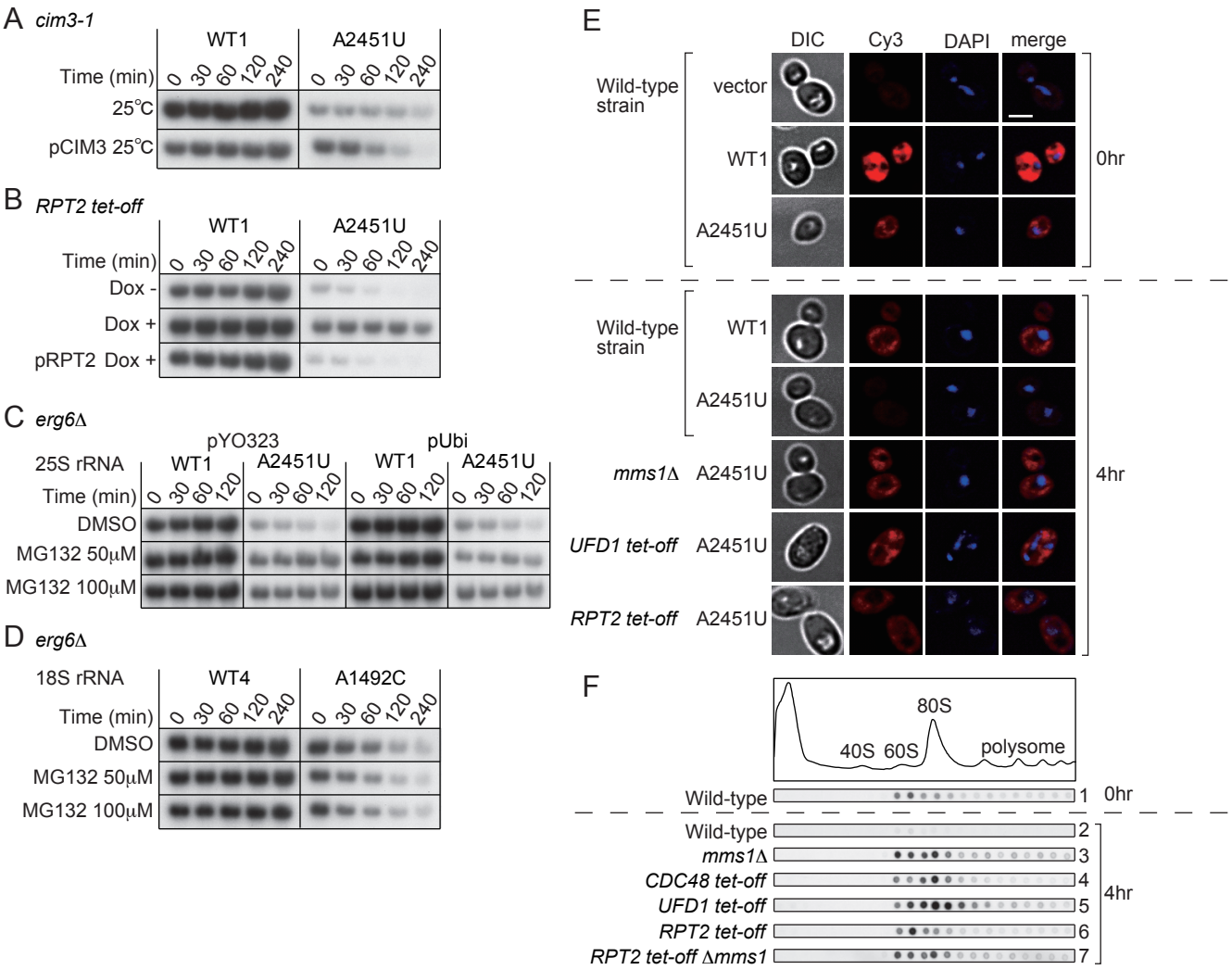

Figure 5 (Kitabatake)

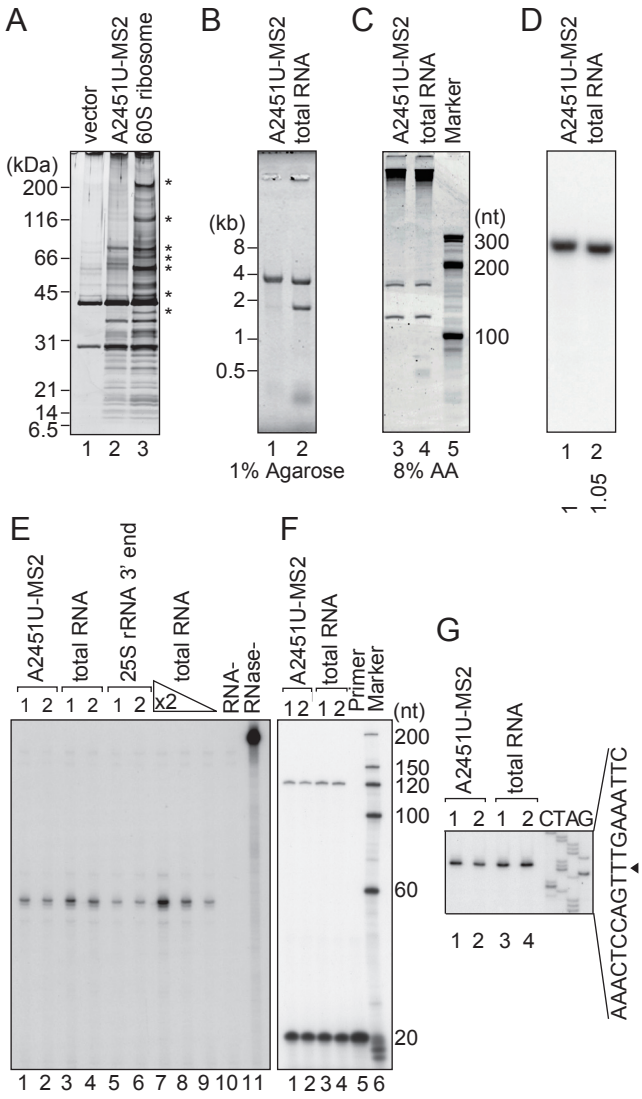

Figure 6 (Kitabatake)

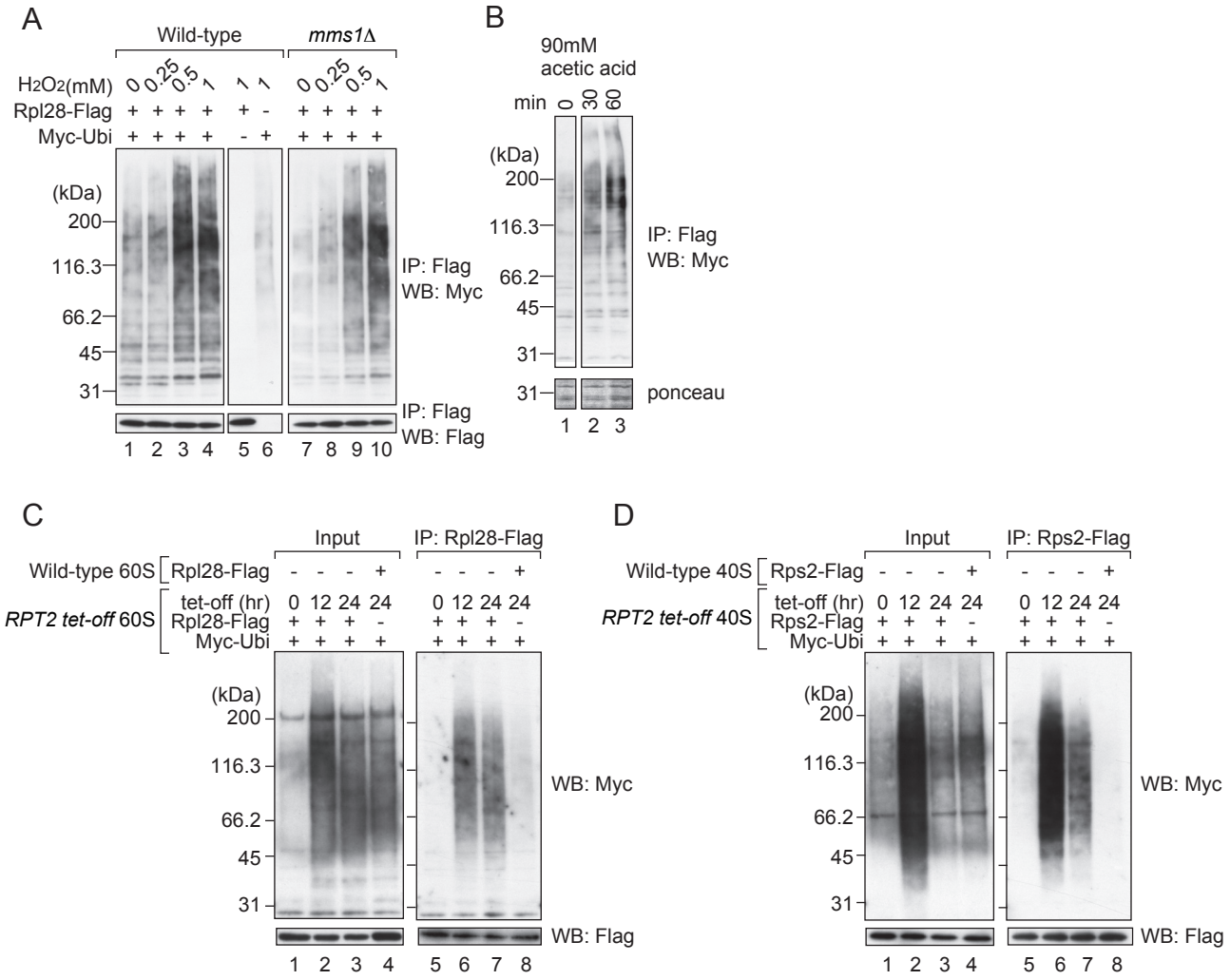

Figure 7 (Kitabatake)

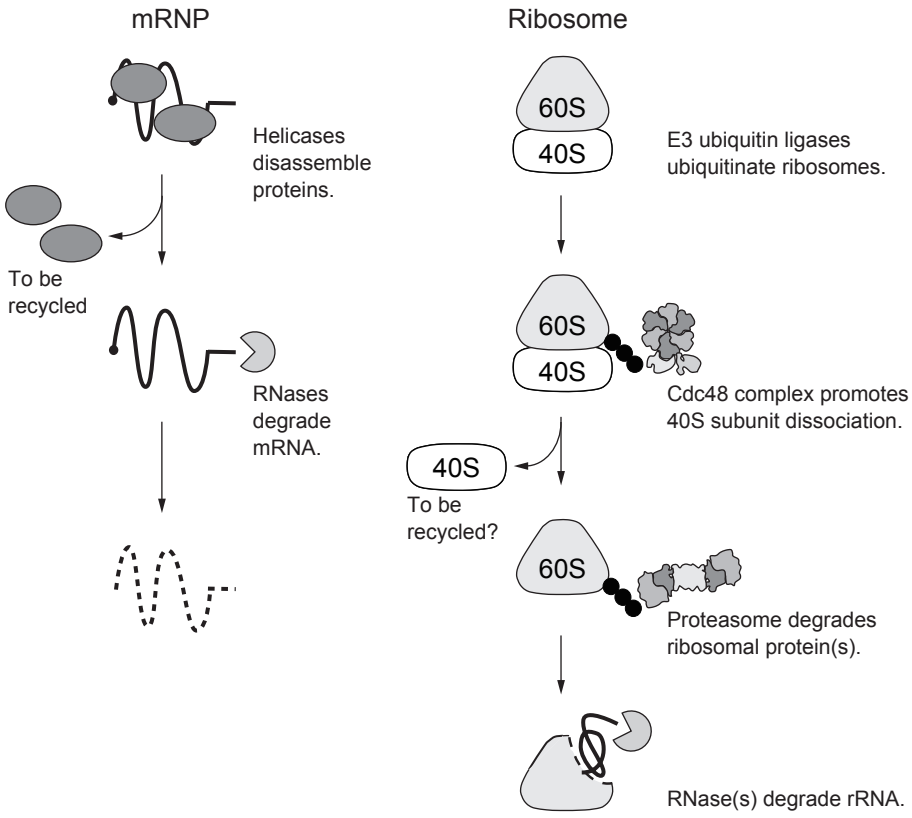

Supplementary Figure S1 (Kitabatake)

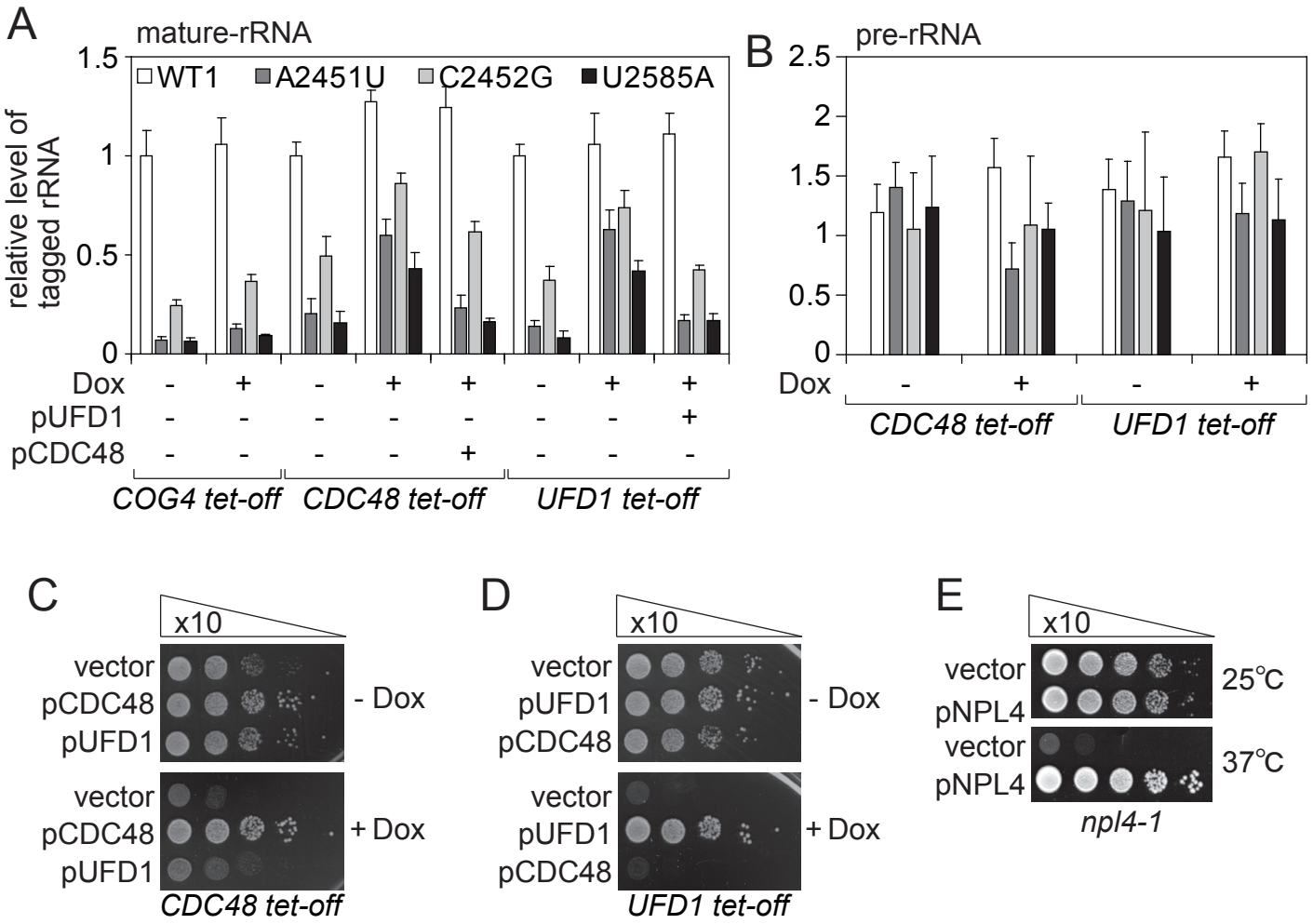

Supplementary Figure S1. Cdc48 complex is involved in the 25S NRD pathway

(A) Quantitative reverse transcription (qRT)–PCR showing the involvement of Cdc48 and Ufd1 in 25S NRD. Nonfunctional 25S rRNAs, A2451U, C2452G, and U2585A, were expressed in tet-off strains. Each mutant strain was collected at A_{600} = 0.5. Total RNAs were purified and examined by qRT–PCR for 25S rRNA containing the 18-nt tag sequence (Supplementary Figure S7B). The *COG4 tet-off* strain was used as a control strain to show that growth repression by the tet-off system did not necessarily induce the accumulation of nonfunctional 25S rRNA. (B) qRT–PCR showing that Cdc48 and Ufd1 are not involved in the accumulation of pre-25S rRNA. The total RNAs purified in (A) were used for qRT–PCR to examine the amounts of pre-25S rRNAs accumulated (Supplementary Figure S7B). The repression of Cdc48 or Ufd1 did not induce the accumulation of pre-25S rRNAs, suggesting that the observed accumulation of nonfunctional 25S rRNAs in (A) is attributable to the inefficient degradation of mature 25S rRNAs. (C) A complementation assay for the *CDC48 tet-off* strain. pCDC48 or pUFD1, a *CEN* plasmid expressing the corresponding gene, was cotransformed into the strain, as indicated. (D) A complementation assay for the *UFD1 tet-off* strain. This was performed as in (C). (E) A complementation assay for the *npl4-1* temperature-sensitive strain. The *npl4-1* strain containing the pNPL4 plasmid or an empty vector was grown at 25 °C and spotted onto YPD plates after serial dilution. The plates were then incubated at the indicated temperatures for 3 days.

Supplementary Figure S2 (Kitabatake)

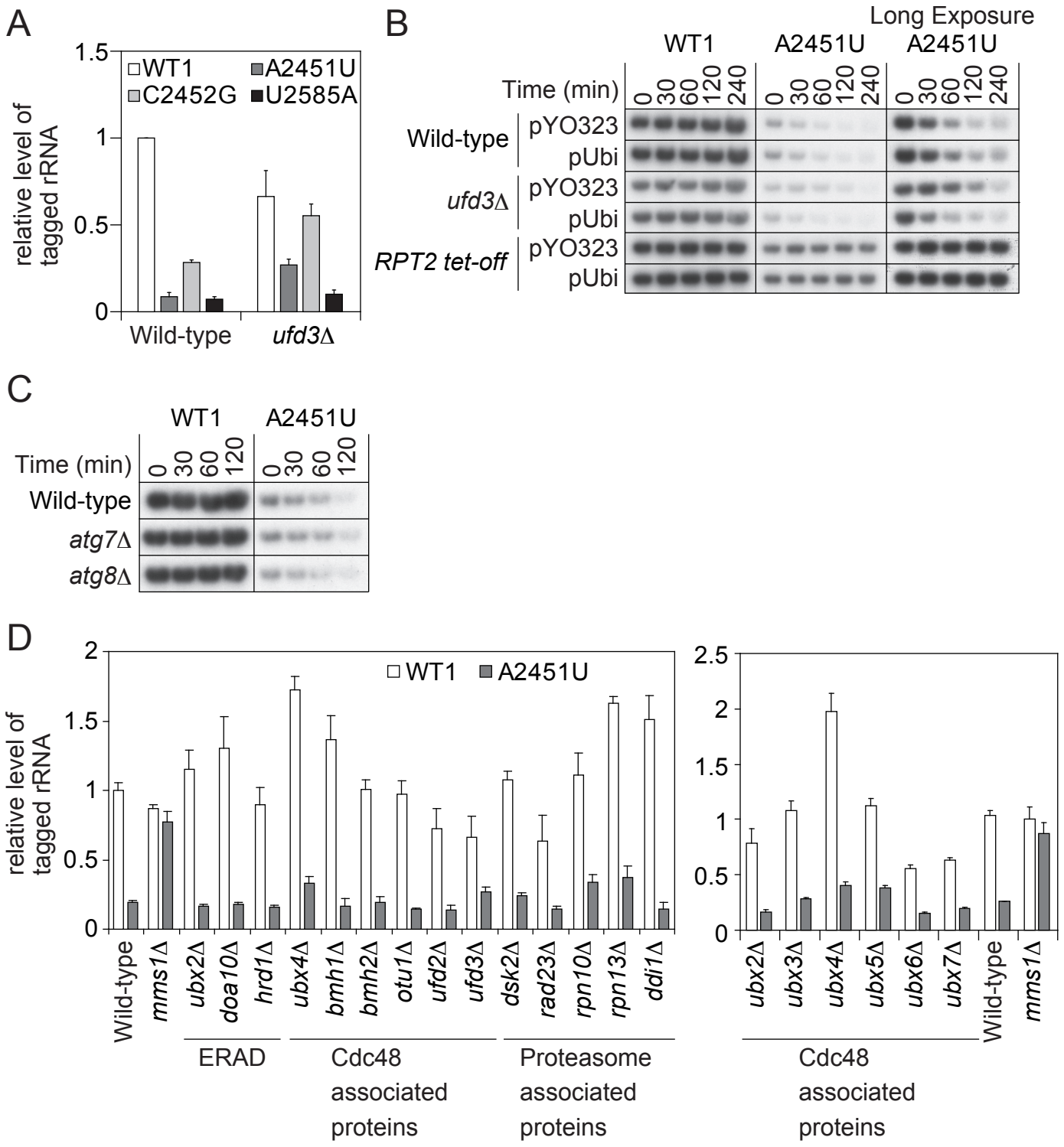

Supplementary Figure S2. Involvement of Cdc48-related factors in 25S NRD was examined

(A) qRT–PCR showing the effects of *UFD3* disruption on 25S NRD. 25S NRD was somewhat inefficient in the *ufd3*Δ strain. The wild-type or *ufd3*Δ strain expressing the indicated 25S rRNA with the 18-nt insertion was harvested and the accumulation of tagged 25S rRNA was measured by qRT–PCR assay. (B) The overexpression of ubiquitin rescued 25S NRD in *ufd3*Δ strain. The indicated strains expressing the 18-nt-tagged wild-type (WT1) or A2451U mutant 25S rRNA (A2451U) with pUbi or empty vector (pYO323), were grown in SD–galactose and the transcription of the tagged rRNAs was shut-off. At the indicated time points, the RNAs were isolated and the tagged RNAs were examined by northern hybridization. $CuSO_4$ was added to the medium 2 h before the medium was changed, to induce the expression of untagged ubiquitin from a *CUP1* promoter in pUbi. (C) Northern blot analysis showing that autophagy is not required for 25S NRD. In *atg7*Δ and *atg8*Δ strains, wild-type (WT1) or nonfunctional mutant (A2451U) 25S rRNA was expressed and the RNAs were prepared and examined as in (B). (D) qRT–PCR assay showing these genes (Carvalho et al, 2006; Richly et al, 2005; Rumpf & Jentsch, 2006; Schuberth et al, 2004; Wang et al, 2009) not involved in 25S NRD. Wild-type (WT1) or nonfunctional mutant (A2451U) 25S rRNA was expressed in the indicated strains and analyzed as in (A). *mms1*Δ is a control strain that lacks a component of E3 ubiquitin ligase essential for 25S NRD.

Supplementary Figure S3 (Kitabatake)

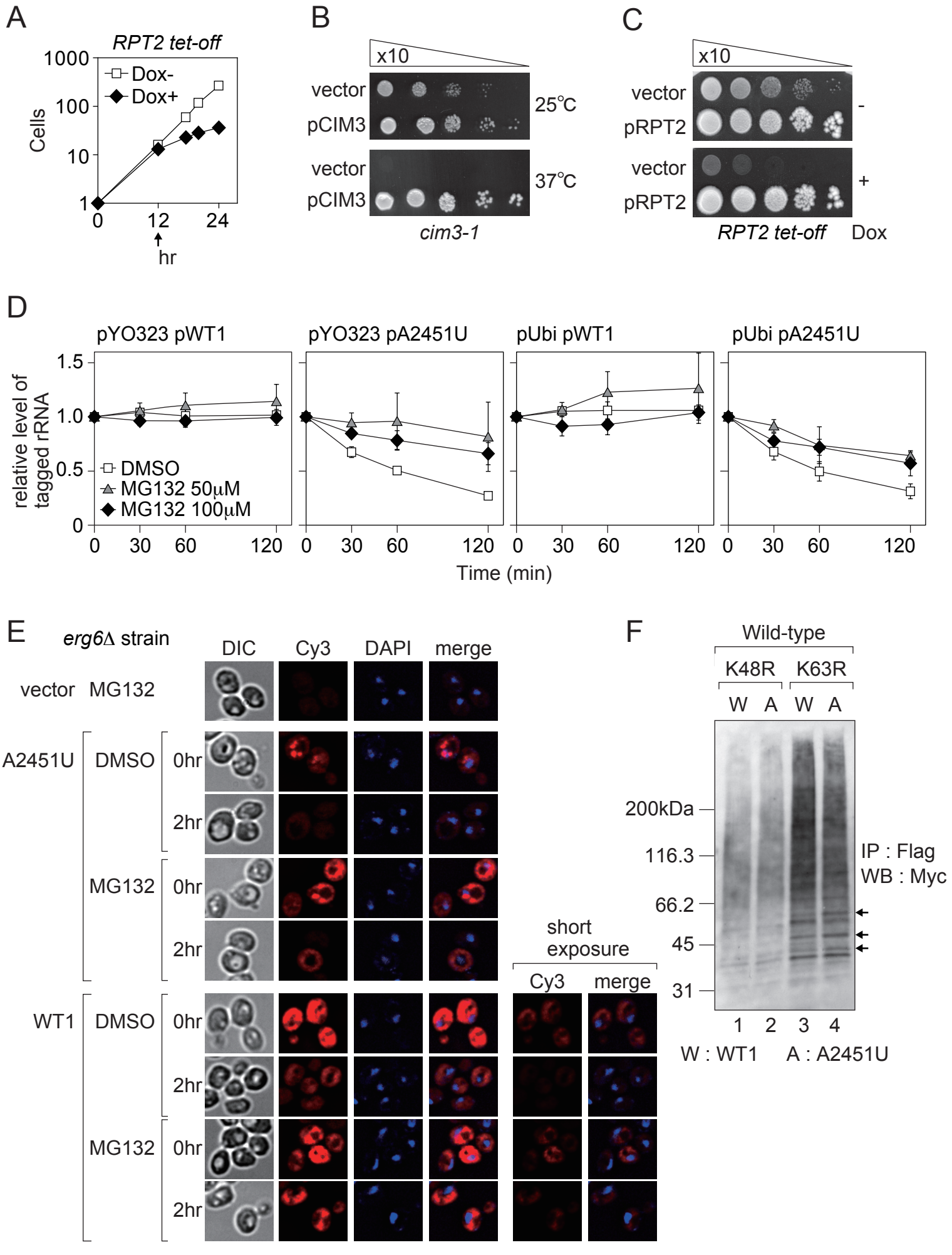

Supplementary Figure S3. Proteasome activity is required for the 25S NRD pathway

(A) Growth curve for the *RPT2 tet-off* strain. The *RPT2 tet-off* strain was grown in SD–glucose medium with or without Dox. The culture was diluted every 12 h to maintain the cells in log phase. A_{600} was monitored at the indicated time points. The arrow indicates the time point at which the cells were harvested for the following analyses. (B) Complementation of *cim3-1* by the pCIM3 plasmid. pCIM3 or an empty vector was introduced into the *cim3-1* strain and grown at 25 °C in SD–glucose. The culture was spotted onto an SD–glucose plate after serial dilution. The plates were incubated for 3 days at 25 °C or 37 °C. (C) Complementation of the *RPT2 tet-off* strain with the pRPT2 plasmid. pRPT2 or an empty vector was introduced into the *RPT2 tet-off* strain, which was grown in SD–glucose. The cultures were spotted onto YPD plates with or without Dox and incubated for 2 days. (D) The stability of nonfunctional rRNA in MG132-treated cells with or without ubiquitin overexpression in Figure 4C was quantified using BAS5000 (FujiFilm). Values are the means ± SD for triplicate experiments. (E) Subcellular localization of an 18-nt-tagged wild-type (WT1) or nonfunctional (A2451U) 25S rRNA in the presence of a proteasome inhibitor. 18-nt-tagged 25S rRNAs were visualized with in situ hybridization using Cy3-labeled oligonucleotide probes. An *erg6*Δ strain was grown in SD–raffinose to A_{600} = 0.5. The medium was then replaced with SD–galactose. The expression of tagged 25S rRNAs was induced for 6 h and the cells were treated with MG132 for 2 h in the same medium. 6 h after induction, the medium was replaced again with SD–glucose containing MG132 or DMSO, and incubated 2 h to shut-off the transcription of the plasmid-derived rRNA. (F) Immunoblot of the ribosomal fractions purified from the wild-type strain expressing

various tagged rRNAs, amino-acid-substituted Myc–ubiquitins, and Rpl28–Flag. Ubiquitinated proteins were probed with anti-Myc antibody. In Myc–ubiquitin, the amino acid encoded by codon 48 (lanes 1 and 2) or 63 (lanes 3 and 4) was changed from lysine to arginine. The arrow indicates the bands enhanced by nonfunctional rRNA expression.

Supplementary Figure S4 (Kitabatake)

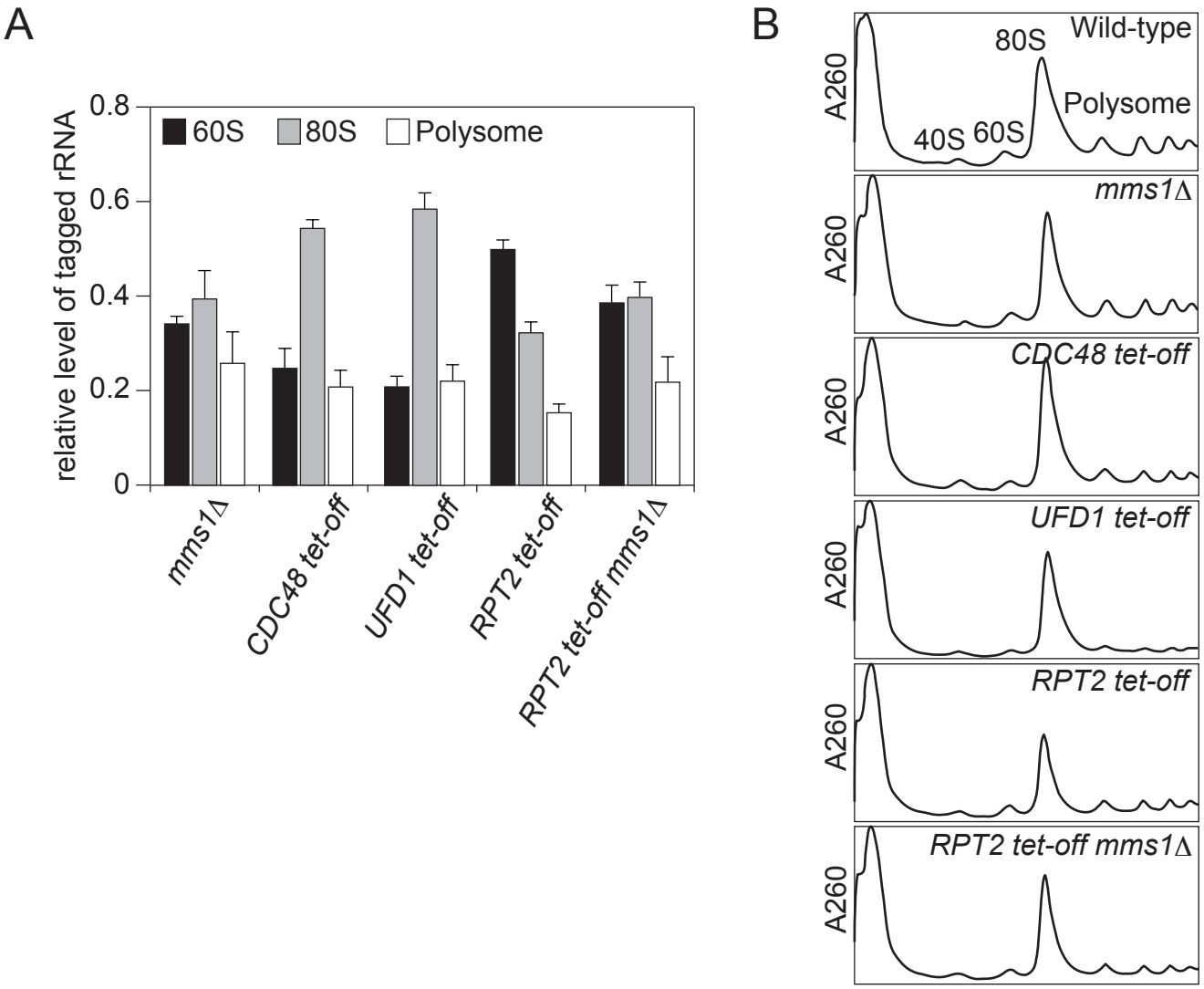

Supplementary Figure S4. Nonfunctional ribosomes accumulated in the 60S fraction in proteasome-deficient cells

(A) The signals for the 60S, 80S, and polysome fractions in Figure 4F were quantified using BAS5000. Values are the means ± SD of triplicate experiments. (B) Polysome profiles of wild-type, *mms1*Δ, *UFD1 tet-off*, *CDC48 tet-off*, *RPT2 tet-off*, and *RPT2 tet-off mms1*Δ strains in Figure 4F were monitored by A_{260}.

Supplementary Figure S5 (Kitabatake)

A

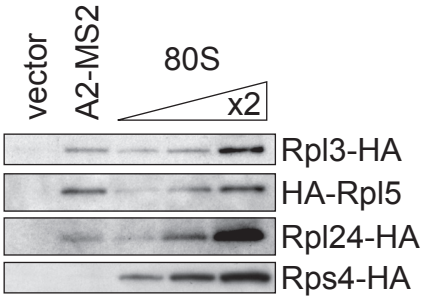

B

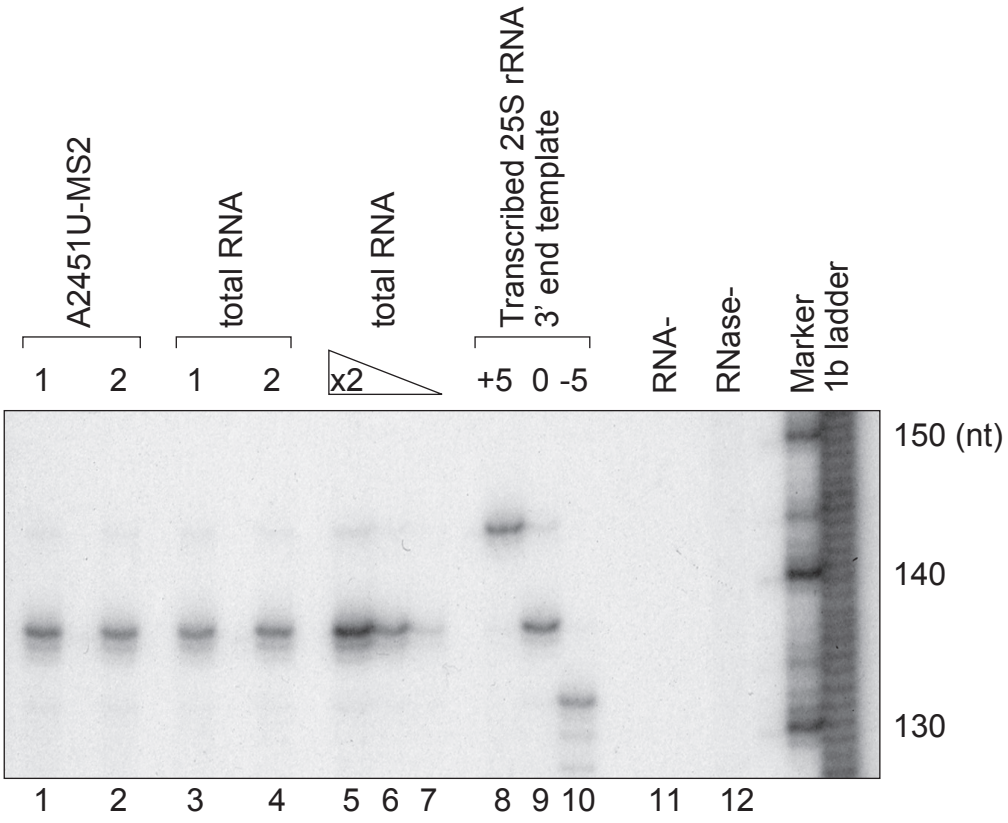

Supplementary Figure S5. Analysis of components of the nonfunctional ribosomes in proteasome-deficient cells

(A) Ribosomal proteins L3, L5, and L24 were retained in the nonfunctional ribosome, which accumulated in the *Rpt2 tet-off* strain. The *Rpt2 tet-off* strain expressing HA-tagged ribosomal proteins, GST–MS2, and MS2-tagged nonfunctional rRNAs was grown in SD–galactose to A_{600} = 0.5. The medium was replaced with SD–glucose and the culture incubated for 4 h to terminate the expression of nonfunctional rRNA. Nonfunctional ribosomes were purified from the 60S fraction with a GST–MS2 pull-down assay and the ribosomal proteins contained were analyzed with anti-HA antibody. As shown in the 80S fraction, the plasmid-derived ribosomal proteins were stably constructed in the ribosome. (B) Nonfunctional 25S rRNA that had accumulated in the proteasome-deficient cells had a perfect 3′ end, at a single-nucleotide resolution, in the same assay as shown Figure 5E. In lanes 1 and 2, purified nonfunctional 25S rRNAs from the *Rpt2 tet-off* strain were used for the RNase protection assay. Total RNA was used as the template in lanes 3–7. The transcribed 3′ region of the 25S rRNA, including +5 nt and –5 nt, was used as the template in lanes 8–10. In lane 11, no target RNA was added to the reaction. Lane 12 is the no-RNase control. The internally labeled marker was produced with in vitro transcription. A single-base ladder was produced with the alkaline hydrolysis of 5′-end-labeled RNA with the same sequence as the probe.

Supplementary Figure S6 (Kitabatake)

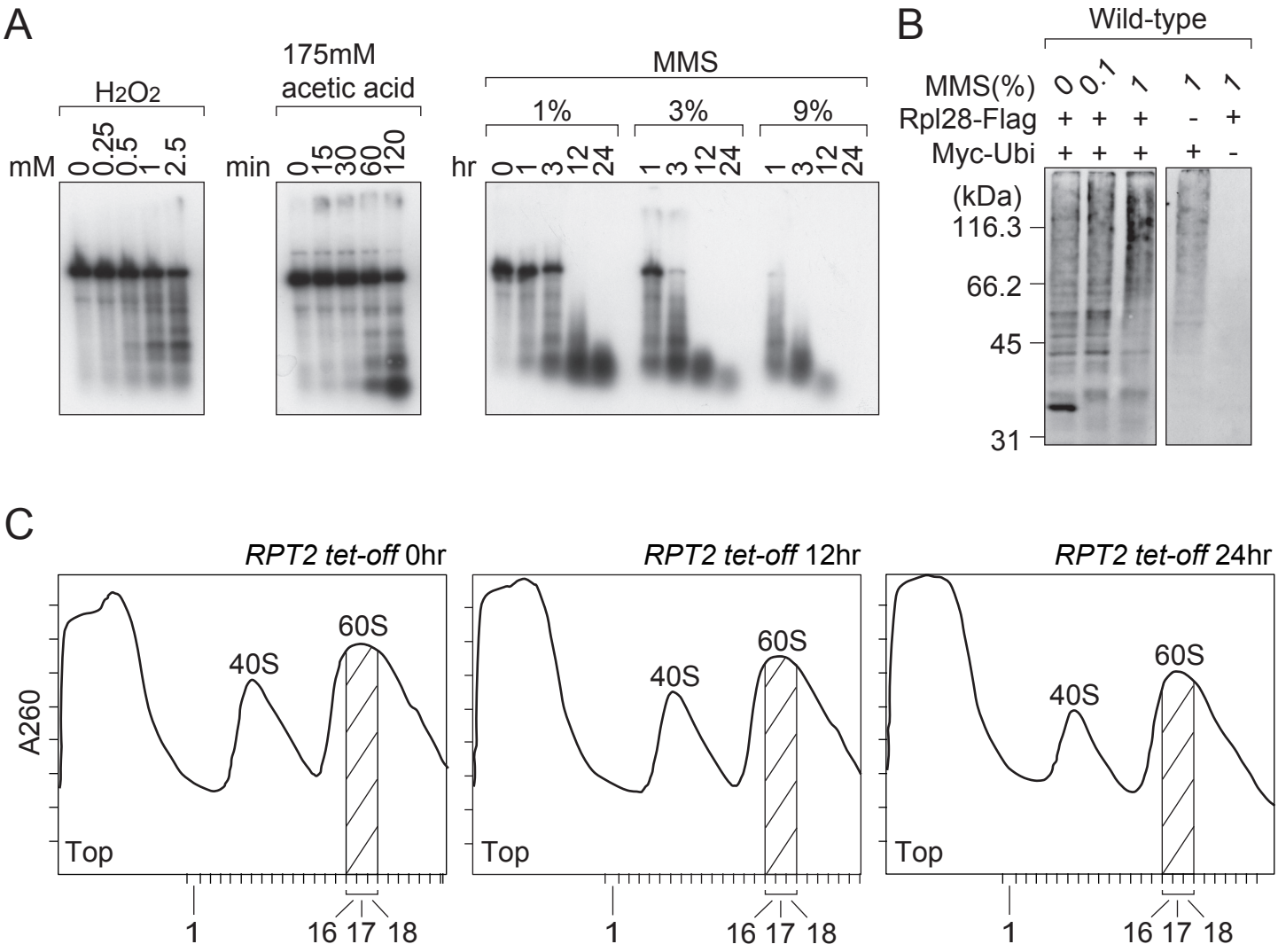

Supplementary Figure S6. Ribosomes are degraded by the ubiquitin–proteasome system

(A) Northern blotting of endogenous 25S rRNA after stress treatments. The wild-type strain was grown in SD–glucose and harvested after the indicated treatments. Total RNAs were isolated from the cells and separated on 1% denaturing agarose. Northern hybridization was performed using the Kota388 probe, which detects endogenous 25S rRNAs. (B) Western blotting of ubiquitinated ribosomes after MMS treatment. pMyc–Ubi and pRpl28–Flag were transformed to the wild-type strain. The transformants were grown in SD–glucose and harvested 2 h after treatment with MMS. The ribosomes were isolated from the strain by immunoprecipitation using anti-Flag agarose. The ubiquitinated proteins were detected with an anti-Myc polyclonal antibody after 12.5% SDS–PAGE. (C) 60S fractions used for the purification in Figure 6C. The *RPT2 tet-off* strain expressing Myc–ubiquitin and Rpl28–Flag were grown in SD–glucose medium containing Dox. The lysates were resolved on a 10%–40% sucrose gradient containing 40 mM EDTA. The fractions indicated were pooled and used as the 60S subunits for immunoprecipitation. Exactly the same result was obtained for the 40S subunit and the wild-type strain.

Supplementary Figure S7 (Kitabatake)

A 18-nt & MS2 tag

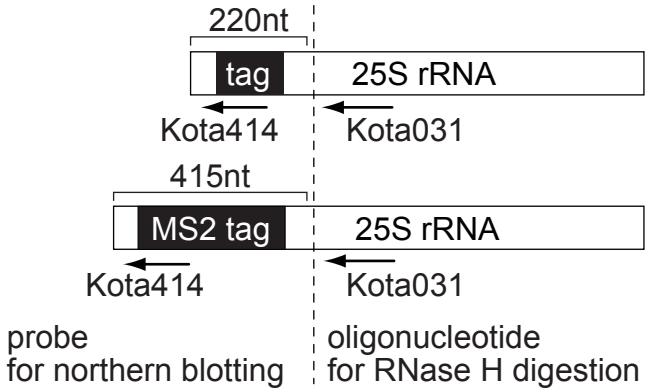

B pre-rRNA or mature rRNA

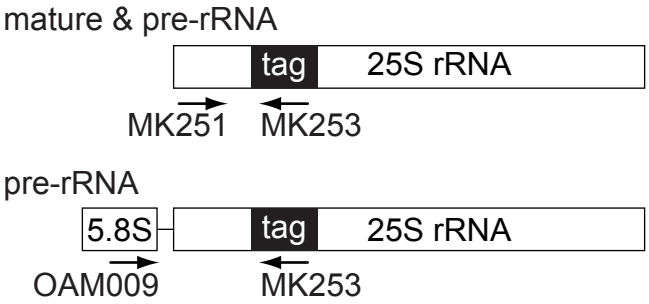

C probe for 3' end

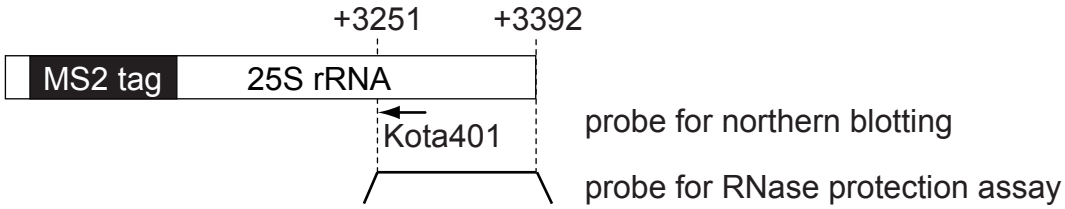

D reverstranscription

Supplementary Figure S7. Primers used for RNA analyses are shown in schematic representation

(A) Oligonucleotides for RNase H digestion and northern blotting (Figure 2A). (B) Primers for qRT–PCR used to measure tagged 25S rRNAs and pre-25S rRNAs (Supplementary Figure S1A and B). (C) Probes for the northern blotting in Figure 5D and the RNase protection assay (Figure 5E and Supplementary Figure S5B). (D) The primer used for the reverse transcription in Figure 5F and G.

Supplementary Methods

Plasmids

pWT1,pA2451U, pC2452G, pU2585A, pWT4, and pA1492C have been described previously (Fujii et al, 2009). To construct pCDC48, pUFD1, pNPL4, pCIM3, and pRPT2, each open reading frame (ORF), including 1 kb each of the upstream and downstream sequences, was amplified by PCR and cloned into YCplac111 (Gietz & Sugino, 1988) or pRS313 (Sikorski & Hieter, 1989).

To construct pRpl28–Flag, pRps2–Flag, pRpl3–HA, Rpl24–HA, and Rps4–HA, the Flag or HA tag was added to the C-terminus of each gene by overlap extension. PCR fragments of each gene, containing the promoter, ORF, tag sequence, and terminator, were cloned into YCplac111 (Gietz & Sugino, 1988) or pRS315 (Sikorski & Hieter, 1989).

To construct pHA–Rpl5, the HA tag was inserted into the N-terminal region at the same position as in the previous paper (Deshmukh et al, 1993) and the endogenous promoter was replaced with the *GAL7* promoter by overlap extension. PCR fragment was cloned into pYO325 (Qadota et al, 1992).

pMyc–UbiK48R and pMyc–UbiK63R were identical to pMyc–Ubi, except for the Lys-to-Arg mutation at codon 48 and 63, respectively.

pWT1–MS2 and pA2451U–MS2 were created by inserting a 195-bp fragment containing 6 repeats of the MS2 coat protein-binding site into the unique *Xho*I site in the 18-nt tag of pWT1 or pA2451U. The inserted fragment

(5′-ctcgagCGTACACCATCAGGGTACGAGCTAGCCCATGGCGTACACCATCAGGGTA
CGACTAGTAGATCTCGTACACCATCAGGGTACGGAAGCTGGTACCTGTACCTTCG

GTGCGTACACCATCAGGGTACGAGCTAGCCCATGGCGTACACCATCAGGGTACGA CTAGTAGATCTCGTACACCATCAGGGTACGctcgag-3′) was amplified with primers MK327 and MK330 using the pδ-crystallin MS2 plasmid as the template (Yoshimoto et al, 2009).

pGST–MS2 was constructed by the assembly of three PCR fragments with overlap extension PCR. These three fragments included 1) the *GPD* promoter amplified by MK331–MK340, 2) the sequence encoding *GST–MS2*, amplified with MK336–MK339, and 3) the *CYC1* terminator amplified with MK337–MK338. MK331 and MK338 were used for the final assembly PCR. The fragment was cloned into pYO325 (Qadota et al, 1992).

Yeast strains and growth conditions

Yeast strain collections, YKO and yTHC, were purchased from Open Biosystems. NOY401 was kindly provided by Dr M. Nomura (Nogi et al, 1991), the *npl4-1* strain was from Dr P. Silver (DeHoratius & Silver, 1996), and the *cim3-1* strain (Ghislain et al, 1993) was obtained from NBRP, Japan. The *TRP1* gene was disrupted by targeting it with a hygromycin-resistance cassette from pFA6 (Goldstein & McCusker, 1999). The same cassette was used to delete the *MMS1* gene in the *RPT2 tet-off* strain from the yTHC collection.

To induce expression from the *GAL7* promoter, the cells were pregrown in SD medium containing 2% raffinose. This culture was inoculated into SD medium containing 2% galactose. The cells were grown until they reached mid-log phase (A_{600} = 0.5). When necessary, the medium was replaced with SD containing 2% glucose to repress the *GAL7* promoter. MG132 was added to the culture medium 2 h before the medium was

changed from 2% galactose to 2% glucose. When ubiquitin overexpression was required, it was achieved by adding 0.1 mM $CuSO_4$ at the same time as MG132. For the Tet-off assay, the yTHC strains were grown in SD medium containing 10 μg/mL Dox (Hughes et al, 2000). The detailed procedures used to screen yTHC are described in the Supplemental Materials. For treatment with H_2O_2, acetic acid, or MMS, the cells were grown in SD medium containing 2% glucose until they reached mid-log phase (A_{600} = 0.5) and were then stressed with H_2O_2 (0.25–1 mM) for 2 h, with 90 mM acetic acid for the indicated time, or with MMS (1%–9%) for the indicated time.

In vivo complementation assay

For the complementation assay, the (pol I ts) NOY401 strain was transformed with a variety of rRNA expressing plasmids. The transformants were pregrown in SD–galactose culture medium at 25 °C, spotted onto a plate in a series of dilutions, and incubated at 25 °C or 37 °C for 3 or 5 days.

Tet-off culture conditions and screening for yTHC

Each tet-off strain showed different sensitivity to Dox treatment, depending upon the stability of the repressed gene product in the strain. To establish the growth conditions for the preparation of factor-depleted cells, we inspected the growth curves of the strains empirically in the presence of Dox. When the cells reached A_{600} = 0.5, they were diluted 20-fold in the same medium containing fresh Dox, to maintain log phase growth. Typically, the culture was diluted every 12 h until the cells ceased to grow. For the analyses, the *UFD1 tet-off*, *RPT2 tet-off*, and *CDC48 tet-off* strains were harvested 12 h, 12 h, and 24 h after Dox treatment, respectively.

To screen the yTHC collection, all 800 yTHC strains were transformed with pA2451U–Leu. The precultured cells grown in 2% galactose medium were diluted 100-fold in the same medium containing 10 μg/mL Dox. After incubation for 24 h, the cells were harvested and spotted onto a membrane, although not all of these strains showed a reduction in growth under these conditions. This membrane was processed with a previously described colony northern technique (Fujii et al, 2009).

Supplementary Tables

Supplementary Table S I , Plasmid list

Plasmid	Notes	Reference	
pNOY102	*URA3*, *2μ*, *GAL7-rDNA*	(Nogi et al, 1991)	pMK001
pWT1	*LEU2*, *2μ*, *GAL7-rDNA 25S-Tag*	(Fujii et al, 2009)	pMK010
pA2451U	*LEU2*, *2μ*, *GAL7-rDNA 25S-Tag A2451U*	(Fujii et al, 2009)	pMK011
pC2452G	*LEU2*, *2μ*, *GAL7-rDNA 25S-Tag C2452G*	(Fujii et al, 2009)	pMK012
pU2585A	*LEU2*, *2μ*, *GAL7-rDNA 25S-Tag U2585A*	(Fujii et al, 2009)	pMK013
pWT4	*URA3*, *2μ*, *GAL7-rDNA 25S-Tag*, *18S-Tag*	(Fujii et al, 2009)	pMK008
pA1492C	*URA3*, *2μ*, *GAL7-rDNA 25S-Tag*, *18S-Tag A1492C*	(Fujii et al, 2009)	pMK009
pWT-MS2	*URA3*, *2μ*, *GAL7-rDNA 25S-MS2 Tag*	This Study	pMK014
pA2451U-MS2	*URA3*, *2μ*, *GAL7-rDNA 25S-MS2 Tag A2451U*	This Study	pMK015
pYO323	*HIS3*, *2μ*	(Qadota et al, 1992)	pMK176
pWT-MS2-His	*HIS3*, *2μ*, *GAL7-rDNA 25S-MS2 Tag*	This Study	pMK016
pA2451U-MS2-His	*HIS3*, *2μ*, *GAL7-rDNA 25S-MS2 Tag A2451U*	This Study	pMK017
pUbi	*HIS3*, *2μ*, *CUP1-Ubi-CYC1*	(Fujii et al, 2009)	pMK089
pMyc-Ubi	*HIS3*, *2μ*, *CUP1-Myc-Ubi-CYC1*	(Fujii et al, 2009)	pMK088
pMyc-UbiK63R	*HIS3*, *2μ*, *CUP1-Myc-UbiK63R-CYC1*	This Study	pMK092
pMyc-UbiK48R	*HIS3*, *2μ*, *CUP1-Myc-UbiK48R-CYC1*	This Study	pMK093
pYO325	*LEU2*, *2μ*	(Qadota et al, 1992)	pMK178
pGST-MS2-Leu	*LEU2*, *2μ*, *GST-MS2*	This Study	pMK151

pRpl28-Flag	*LEU2, 2μ, RPL28-Flag*	This Study	pMK077
pRS315	*LEU2, CEN*	(Sikorski & Hieter, 1989)	pMK196
pRps2-Flag	*LEU2, CEN, RPS2-Flag*	This Study	pMK231
pRps4-HA	*LEU2, CEN, RPS4-HA*	This Study	pMK038
pRpl3-HA	*LEU2, CEN, RPL3-HA*	This Study	pMK042
pHA-Rpl5	*LEU2, 2μ, GAL7-HA-RPL5*	This Study	pMK200
pRpl24-HA	*LEU2, CEN, RPL24-HA*	This Study	pMK047
pYO324	*TRP1*, *2μ*	(Qadota et al, 1992)	pMK177
pGST-MS2-Trp	*TRP1*, *2μ*, *GST-MS2*	This Study	pMK153
pRS313	*HIS3*, *CEN*	(Sikorski & Hieter, 1989)	pMK195
pCDC48	*HIS3*, *CEN*, *CDC48*	This Study	pMK133
pUFD1	*HIS3*, *CEN*, *UFD1*	This Study	pMK139
pRPT2	*HIS3*, *CEN*, *RPT2*	This Study	pMK143
YCplac111	*LEU2*, *CEN*, *lacZ*	(Gietz & Sugino, 1988)	pMK169
pNPL4	*LEU2*, *CEN*, *NPL4*	This Study	pMK144
pCIM3	*LEU2*, *CEN*, *CIM3*	This Study	pMK142
pAG26	*hphMX6*, *CEN*, *URA3*	(Goldstein & McCusker, 1999)	pMK179

Supplementary Table SⅡ, Yeast Strains list

Strain	Genotype and Notes	Reference	
BY20693	*MATa, his3-1, leu2-Δ0, ura3-Δ0*	(Brachmann et al, 1998)	MKY13
mms1Δ	*MATa, his3-1, leu2-Δ0, ura3-Δ0, met15Δ0, mms1Δ::KanMX4*	(Winzeler et al, 1999)	MKY47
NOY401	*MATa, rpa190-3, ura3, leu2, trp1, can1*	(Nogi et al, 1991)	MKY7
CYH2-Flag	*MATa, his3-1, leu2-Δ0, ura3-Δ0, RPL28-CYH2-Flag*	(Fujii et al, 2009)	MKY17
CYH2-Flag, mms1Δ	*MATa, his3-1, leu2-Δ0, ura3-Δ0, RPL28-CYH2-Flag, mms1Δ::KanMX4*	(Fujii et al, 2009)	MKY18
CYH2-Flag, trp1Δ	*MATa, his3-1, leu2-Δ0, ura3-Δ0, RPL28-CYH2-Flag, trp1Δ::hphMX6*	This Study	MKY137
CDC48 tet-off	*MATa, his3-1, leu2-Δ0, ura3-Δ0, URA3::CMV-tTA, KanMX::tetO$_7$CYC$_{TATA}$CDC48*	(Hughes et al, 2000)	MKY69
CDC48 tet-off, mms1Δ	*MATa, his3-1, leu2-Δ0, ura3-Δ0, URA3::CMV-tTA, KanMX::tetO$_7$CYC$_{TATA}$CDC48, mms1Δ::hphMX6*	This Study	MKY70
UFD1 tet-off	*MATa, his3-1, leu2-Δ0, ura3-Δ0, URA3::CMV-tTA, KanMX::tetO$_7$CYC$_{TATA}$UFD1*	(Hughes et al, 2000)	MKY37
PSY825	*MATa, ura3-52, leu2Δ1, npl4-1*	(DeHoratius & Silver, 1996)	MKY64
RPT2 tet-off	*MATa, his3-1, leu2-Δ0, ura3-Δ0, URA3::CMV-tTA, KanMX::tetO$_7$CYC$_{TATA}$RPT2*	(Hughes et al, 2000)	MKY92

RPT2 tet-off, mms1Δ	*MATa, his3-1, leu2-Δ0, ura3-Δ0, URA3::CMV-tTA, KanMX:: $tetO_7CYC_{TATA}RPT2$, mms1Δ::hphMX6*	This Study	MKY108
cim3-1	*MATα cim3-1 ura3-52 leu2-Δ1*	(Ghislain et al, 1993)	MKY70
erg6Δ	*MATa, his3-1, leu2-0, ura3-Δ0, met15Δ0, erg6Δ::KanMX4*	(Winzeler et al, 1999)	MKY34

Supplementary Table SⅢ, Oligo list

Name	Sequence	Notes
OAM009	5'-AGGGGGCATGCCTGTTGAG	5.8S rRNA sequence
MK251	5'-GACCTCAAATCAGGTAGGAG TACCC	25S rRNA sequence
MK253	5'-CACCGAAGGTACACTCGAGA GCTTC	complementary to pWT1, pWT4 25S rRNA tag sequence
Kota030	5'-GAAATCTGGTACCTTCGGTG	untagged 25S rRNA sequence
Kota031	5'-GATTCTCACCCTCTATGACG	complementary to untagged 25S rRNA sequence
Kota153	5'-CGAGGATTCAGGCTTTGG	complementary to pWT4 18S tagged sequence
Kota414	5'-GTACACTCGAGAGCTTCAGT ACCAC	prove for MS2 tag & 18nt tag sequence
Kota401	5'-GACATTGCAATTCGCCAGCA AGCA	complementary to 25S rRNA sequence
Kota379	5'-GATGACTAGCTTGCTGGCGA ATTGCAATGTC	fw prime for the template of RPA probe *in vitro* transcription
Kota383	5'-TAATACGACTCACTATAGGG AGA tcctgccagtacccacttagaaag	rev prime for the template of RPA probe *in vitro* transcription
Kota381	5'-TAATACGACTCACTATAGGG AGA tgcttgctggcgaattgcaatgtc	rev prime for the template of 25S rRNA 3' region *in vitro* transcription
Kota382	5'-ACAAATCAGACAACAAAGGC	complementary to 25S rRNA sequence
Kota380	5'-GTACCAGATTTCAAATTTGAG C	complementary to 25S rRNA sequence
Kota388	5'-TTCCTCCGCTTATTGATATGC	complementary to 25S rRNA 5' reagion
Kota179	5'-ATCTTCCTCATCGTCTTCAG	upstream sequence of the *UFD1* gene
Kota182	5'-TCCAGCATCCTAATGTGCAC	complementary sequence to downstream of the *UFD1* gene
Kota219	5'-CACCAATGATGGCGATAGTC	upstream sequence of the *CDC48* gene
Kota220	5'-ACATGTCTCTCGCCATTCTTG	complementary sequence to

		downstream of the *CDC48* gene
Kota221	5’-TCTGCTGCTGGTGGTTATCC	upstream sequence of the *CIM3* gene
Kota222	5’-ACGTTCACCAGTTTTCGTAG	complementary sequence to downstream of the *CIM3* gene
Kota357	5’-GATTGCACCTATTGCAGAAG	upstream sequence of the *RPT2* gene
Kota358	5’-GTCATATGGTGTTTCTGGCC	complementary sequence to downstream of the *RPT2* gene
Kota213	5’-CACACAGTAGGCACTAATTG	upstream sequence of the *NPL4* gene
Kota214	5’-TCGTTGACAATCCTTACAGG	complementary sequence to downstream of the *NPL4* gene
Kota488	5’-TC GGTATCTCAG CATCTAGG	upstream sequence of the *RPS2* gene
Kota535	5’- GAT TAC AAG GAC GAC GAT GAC AAG taagcttgttgtctacaaattataaaatag	construction of pRps2-Flag
Kota532	5’-CTT GTC ATC GTC GTC CTT GTA ATC gaatctcttcttttgagcagaagc	construction of pRps2-Flag
Kota472	5’-AACAATGTAA GTTCGGTACG	complementary sequence to downstream of the *RPS2* gene
MK704	5-CACTTACGTTATCATTCTAAA G	upstream sequence of the *RPL3* gene
MK705	5-ctacgcatagtcaggaacatcgtatgggta caagtccttcttcaaagtacc	construction of pRpl3-HA
MK714	5-GCTGTTGCTATTGCCAAGTTA AG	upstream sequence of the *RPL24* gene
MK715	5-ctacgcatagtcaggaacatcgtatgggta acgagaagtagcagcaacctttg	construction of pRpl24-HA
MK696	5-CTAATGGAGAGCTGGGTACTG C	upstream sequence of the *RPS4* gene
MK697	5-ctacgcatagtcaggaacatcgtatgggta taaaccttgttgagctcttcttctg	construction of pRps4-HA
MK722	5-CATACGATGTTCCTGACTATG CGtagATCTAAAAACTTCATCAA AG	HA tag and *RPL13* gene 3' UTR sequence

MK395	5-ttcatacattcttaaattgc	upstream sequence of the *GAL7* gene
MK685	5-tatccctatgacgtcccggactatgcaTCCTCTGCTTACTCCTCTCGTTTC	construction of pHA-Rpl5
MK686	5-tgcatagtccgggacgtcatagggatacttagcgtctttttggaaagccat	construction of pHA-Rpl5
MK687	5-gttagaatgccattctagag	complementary sequence to downstream of *RPL5* gene
MK723	5-ccaaaacttgaaggacttattgg	complementary sequence to downstream of the *RPL13* gene
MK327	5-acatcagctttaagCTCGAG	Used for amplifying MS2 tag sequence
MK330	5-aacatttccgtgtcctcgag	Used for amplifying MS2 tag sequence
MK331	5-GCGGCCGCacacgctttttcagttcgag	Used for amplifying *GPD* promoter fragment
MK336	5-caatgtgggatccacctgttttagtagatgccggagtttg	Used for amplifying GST-MS2 fragment
MK337	5-AACAGGTGGATCCCACATTGtcatgtaattagttatgtcac	Used for amplifying *CYC1* terminator fragment
MK338	5-ggtatcctcgagggccgcaaattaaagcctc	Used for amplifying *CYC1* terminator fragment
MK339	5-gtttcgaataaacacacataaacaaacaaaATGtcccctatactaggttattg	Used for amplifying GST-MS2 fragment
MK340	5-caataacctagtataggggacattttgtttgttatgtgtgtttattcgaaac	used for amplifying *GPD* promoter fragment
MK590	5-atctttgccggtAGAcagctcgaggac	construction of pMyc-UbiK48R
MK591	5-gtcctcgagctgtctaccggcaaagat	construction of pMyc-UbiK48R
MK592	5-attacaacattcagAGAgagtcgaccttac	construction of pMyc-UbiK63R
MK593	5-gtaaggtcgactctctctgaatgttgtaat	construction of pMyc-UbiK63R
MK560	5-aacaagcgctcatgagcccg	upstream sequence of the Myc-Ubi *CUP1* promoter
MK561	5-gacagcttatcatcgataag	complementary sequence to downstream of the Myc-Ubi *CYC1* terminator

Supplementary References

Brachmann CB, Davies A, Cost GJ, Caputo E, Li J, Hieter P, Boeke JD (1998) Designer deletion strains derived from Saccharomyces cerevisiae S288C: a useful set of strains and plasmids for PCR-mediated gene disruption and other applications. *Yeast* **14:** 115-132

Carvalho P, Goder V, Rapoport TA (2006) Distinct ubiquitin-ligase complexes define convergent pathways for the degradation of ER proteins. *Cell* **126:** 361-373

DeHoratius C, Silver PA (1996) Nuclear transport defects and nuclear envelope alterations are associated with mutation of the Saccharomyces cerevisiae NPL4 gene. *Mol Biol Cell* **7:** 1835-1855

Deshmukh M, Tsay YF, Paulovich AG, Woolford JL Jr (1993) Yeast ribosomal protein L1 is required for the stability of newly synthesized 5S rRNA and the assembly of 60S ribosomal subunits. *Molecular and cellular biology* **13:** 2835-2845

Fujii K, Kitabatake M, Sakata T, Miyata A, Ohno M (2009) A role for ubiquitin in the clearance of nonfunctional rRNAs. *Genes Dev* **23:** 963-974

Ghislain M, Udvardy A, Mann C (1993) S. cerevisiae 26S protease mutants arrest cell division in G2/metaphase. *Nature* **366:** 358-362

Gietz RD, Sugino A (1988) New yeast-Escherichia coli shuttle vectors constructed with in vitro mutagenized yeast genes lacking six-base pair restriction sites. *Gene* **74:** 527-534

Goldstein AL, McCusker JH (1999) Three new dominant drug resistance cassettes for gene disruption in Saccharomyces cerevisiae. *Yeast* **15:** 1541-1553

Hughes TR, Marton MJ, Jones AR, Roberts CJ, Stoughton R, Armour CD, Bennett HA, Coffey E, Dai H, He YD, Kidd MJ, King AM, Meyer MR, Slade D, Lum PY, Stepaniants SB, Shoemaker DD, Gachotte D, Chakraburtty K, Simon J, Bard M, Friend SH (2000) Functional discovery via a compendium of expression profiles. *Cell* **102:** 109-126

Nogi Y, Yano R, Nomura M (1991) Synthesis of large rRNAs by RNA polymerase II in mutants of Saccharomyces cerevisiae defective in RNA polymerase I. *Proc Natl Acad Sci U S A* **88:** 3962-3966

Qadota H, Ishii I, Fujiyama A, Ohya Y, Anraku Y (1992) RHO gene products, putative small GTP-binding proteins, are important for activation of the CAL1/CDC43 gene product, a protein geranylgeranyltransferase in Saccharomyces cerevisiae. *Yeast* **8:** 735-741

Richly H, Rape M, Braun S, Rumpf S, Hoege C, Jentsch S (2005) A series of ubiquitin binding factors connects CDC48/p97 to substrate multiubiquitylation and proteasomal targeting. *Cell* **120:** 73-84

Rumpf S, Jentsch S (2006) Functional division of substrate processing cofactors of the ubiquitin-selective Cdc48 chaperone. *Mol Cell* **21:** 261-269

Schuberth C, Richly H, Rumpf S, Buchberger A (2004) Shp1 and Ubx2 are adaptors of Cdc48 involved in ubiquitin-dependent protein degradation. *EMBO Rep* **5:** 818-824

Sikorski RS, Hieter P (1989) A system of shuttle vectors and yeast host strains designed for efficient manipulation of DNA in Saccharomyces cerevisiae. *Genetics* **122**: 19-27

Wang Y, Meriin AB, Zaarur N, Romanova NV, Chernoff YO, Costello CE, Sherman MY (2009) Abnormal proteins can form aggresome in yeast: aggresome-targeting signals and components of the machinery. *FASEB J* **23**: 451-463

Winzeler EA, Shoemaker DD, Astromoff A, Liang H, Anderson K, Andre B, Bangham R, Benito R, Boeke JD, Bussey H, Chu AM, Connelly C, Davis K, Dietrich F, Dow SW, El Bakkoury M, Foury F, Friend SH, Gentalen E, Giaever G, Hegemann JH, Jones T, Laub M, Liao H, Liebundguth N, Lockhart DJ, Lucau-Danila A, Lussier M, M'Rabet N, Menard P, Mittmann M, Pai C, Rebischung C, Revuelta JL, Riles L, Roberts CJ, Ross-MacDonald P, Scherens B, Snyder M, Sookhai-Mahadeo S, Storms RK, Veronneau S, Voet M, Volckaert G, Ward TR, Wysocki R, Yen GS, Yu K, Zimmermann K, Philippsen P, Johnston M, Davis RW (1999) Functional characterization of the S. cerevisiae genome by gene deletion and parallel analysis. *Science* **285**: 901-906

Yoshimoto R, Kataoka N, Okawa K, Ohno M (2009) Isolation and characterization of post-splicing lariat-intron complexes. *Nucleic Acids Res* **37**: 891-902